

UNITED STATES DEPARTMENT OF THE INTERIOR
GEOLOGICAL SURVEY

Geomorphology and Glacial Geology

Wolverton and Crescent Meadow Areas and Vicinity

Sequoia National Park, California

by Clyde Wahrhaftig¹

with a section on the Geology of Emerald Lake basin

in relation to acid precipitation

by James G. Moore¹ and Clyde Wahrhaftig

and a section on Seismic Refraction studies

of the Thickness of Alluvium in the

Wolverton Ground-water Basin

and beneath Crescent Meadow

by John C. Tinsley¹

Open-file Report 84-400

Prepared in cooperation with the National Park Service

This report is preliminary and has not been reviewed for conformity with U. S. Geological
Survey editorial standards and stratigraphic nomenclature.

¹. Menlo Park, California, 94025

1984

Table of Contents

Introduction and acknowledgements	1
Geomorphology of the Kaweah Basin, Sequoia National Park	4
The stepped topography	5
Geomorphic evolution of the Kaweah drainage in the light of stepped topography	9
Glacial geology	13
Glaciers	13
Glacial erosion	24
Glacial deposits	15
The record of Pleistocene Glaciations	16
Glacial geology of the Wolverton-Lodgepole area	23
Volume of the Wolverton ground-water basin	26
Surficial geology and geomorphology of the Crescent Creek basin in relation to acid precipitation	30
Geology of Emerald Lake basin in relation to acid precipitation, by James G. Moore and Clyde Wahrhaftig	36
Seismic Refraction Studies of the Thickness of Alluvium in the Wolverton Ground-water Basin and beneath Crescent Meadow, by John C. Tinsley	40
References Cited	48

List of Illustrations

Plate 1	Geologic map of the Giant Forest-Lodgepole area, Sequoia National Park, California, by Thomas W. Sisson, James G. Moore, and Clyde Wahrhaftig	
Plate 2	Map of the Wolverton water-supply area, Sequoia National Park, by Clyde Wahrhaftig, Richard G. Luginbuhl, and Jay Akers	
Figure 1	Map of the western part of Sequoia National Park, and vicinity, showing locations of Plates 1 and 2 and Figures 7, 8, and 9, and the areas of the three topographic types described in the text	3
Figure 2	Stages in the development of stepped topography	11
Figure 3	The mountain ice-cap of the Sierra Nevada and neighboring valley and cirque glaciers at the height of Tahoe glaciation	12
Figure 4	Correlation chart of climatic events and deposits in the Sierra Nevada, San Joaquin Valley, Searles Lake, and in Deep Sea Cores	21
Figure 5	Vertical cross-sections of the alluvial basin at Wolverton, Sequoia National Park	27
Figure 6	Contours on thickness of alluvial fill in the basin at Wolverton, Sequoia National Park	28
Figure 7	Photogeologic map of bedrock outcrops and wet meadows on the Giant Forest plateau, Sequoia National Park, California	31
Figure 8	Bedrock geology of the Emerald Lake cirque and vicinity, Sequoia National Park, by James G. Moore	38
Figure 9	Surficial photogeologic reconnaissance map of Emerald Lake and vicinity, Sequoia National Park	39
Figure 10	Diagrams illustrating the principles of refraction seismic measurements of depth to bedrock	44

Tables

Table 1	Calculation of volume of alluvium in the Wolverton ground-water basin	29
Table 2	Mineral composition of thin-sections from the Giant Forest pluton	32
Table 3	Chemical formulas and abrasion pH of minerals that may be present in weathered granodiorite	35
Table 4	Data and interpretation of seismic surveys in the Wolverton and Crescent Meadow areas	45

GEOMORPHOLOGY AND GLACIAL GEOLOGY
WOLVERTON AND CRESCENT MEADOW AREAS AND VICINITY
SEQUOIA NATIONAL PARK
CALIFORNIA

by Clyde Wahrhaftig
with a section on the Geology of Emerald Lake basin
in relation to acid precipitation
by James G. Moore and Clyde Wahrhaftig
and a section on Seismic Refraction Studies
of the Thickness of Alluvium in the
Wolverton Ground-water Basin
and beneath Crescent Meadow
by John C. Tinsley

Introduction and Acknowledgements

This report on the Geomorphology and Glacial Geology of the Wolverton and Crescent Meadow areas and vicinity is partial fulfillment of an agreement between the Geological Survey and the National Park Service to provide geologic information on part of Sequoia Park for water-supply and other purposes. As written, this report is designed to fill three needs:

(1) To provide geologic background for an assessment of the ground-water potential of the Wolverton basin and of the impact of withdrawing water from that basin on the drainage basin of Sherman Creek. This material is provided in the section on Volume of the Wolverton Ground-water Basin and in Seismic Refraction Studies of the Thickness of Alluvium in the Wolverton Ground-water Basin and beneath Crescent Meadow.

(2) To provide geologic background relevant to the use of the drainage basins above the lower end of Crescent Meadow and of the cirque containing Emerald Lake for monitoring the effect of atmospheric pollution and acid precipitation on Sequoia National Park. This material is presented in the sections on Surficial Geology and Geomorphology of Cresecent Creek basin in relation to acid precipitation and Geology of Emerald Lake basin in relation to acid precipitation.

(3) To provide background information on the evolution of the landscape of the Giant Forest—Lodgepole area of Sequoia National Park for the use of the interpretive ranger staff of the park. This information is presented in the sections on Geomorphology of the Kaweah Basin and Glacial Geology. These are the two longest parts of the report, because an attempt was made to write them to be clearly understood by persons of normal college education who have not had any training in geology. Much background material had to be included to clarify the relation of the evidence in the Sierra Nevada and the events inferred therefrom to our knowledge of, for example, glacial advances in other parts of the world. These two sections are also useful background for understanding the other parts of the report.

Jay Akers and I made a three-day trip to Sequoia Park on July 6—8, 1983, to acquaint ourselves with the nature of the problem and the needs of the Park Service. Because of heavy snowpack throughout the Sierra Nevada during the early summer and because of commitments to work elsewhere, field work could not begin until about the first of September. I spent the periods Aug. 31—Sept. 4 and Sept. 14—18 in the Park, mapping glacial geology. Tom Sisson and Dan Duriscoe accompanied me on Sept. 1 and 2,

respectively, and John C. Tinsley spent Sept. 14— 16 making the seismic surveys, assisted by Gary Collier and me. Jay Akers and I returned to the Park to make a control plane-table survey of the Wolverton area for a photogrammetric map, during Nov. 9—11. Dates given include travel to and from the park.

Approximately five and one-half days were spent in December, 1983, preparing the map of the Wolverton ground-water area (Plate 2) and writing an early draft of the report, and 46 days in January—March, 1984, completing the report, doing photogeology of the Crescent Creek and Emerald Lake areas, and drafting the illustrations.

Beside Thomas Sisson, James G. Moore, Jay Akers, and John C. Tinsley, the other authors of this and the accompanying reports, the following persons provided assistance: Of the National Park Service, Ken Bachmeyer, Larry Bancroft, Steve Barnes, Dan Duriscoe, David Graber, Kathy Kovell, David Parsons, William Tweed, Dawn Vernon, Tom Warner, and Harold Werner. Of the U. S. Geological Survey, Richard Lugin set up the photogrammetric model for Plate 2; Fidelia Portillo, Jaylynn M. L. Chun, and Barbara Bernegger provided assistance with the drafting; Christopher G. Utter did photographic reproductions for the report; Stacey Andrews, John Galloway, and Dorothy De Mar instructed me on the use of the word processor; and David P. Adam, Charles Bacon, Edward J. Helley, Andre Sarna-Wojcicki, and George I. Smith provided provided scientific information on ^{14}C Dating, the Great Valley of California, Owens Valley, and Searles Lake. I am especially grateful to Gary Collier for providing transportation on two trips to the park, company in the field, and the muscles to power the hammer-driven seismograph.

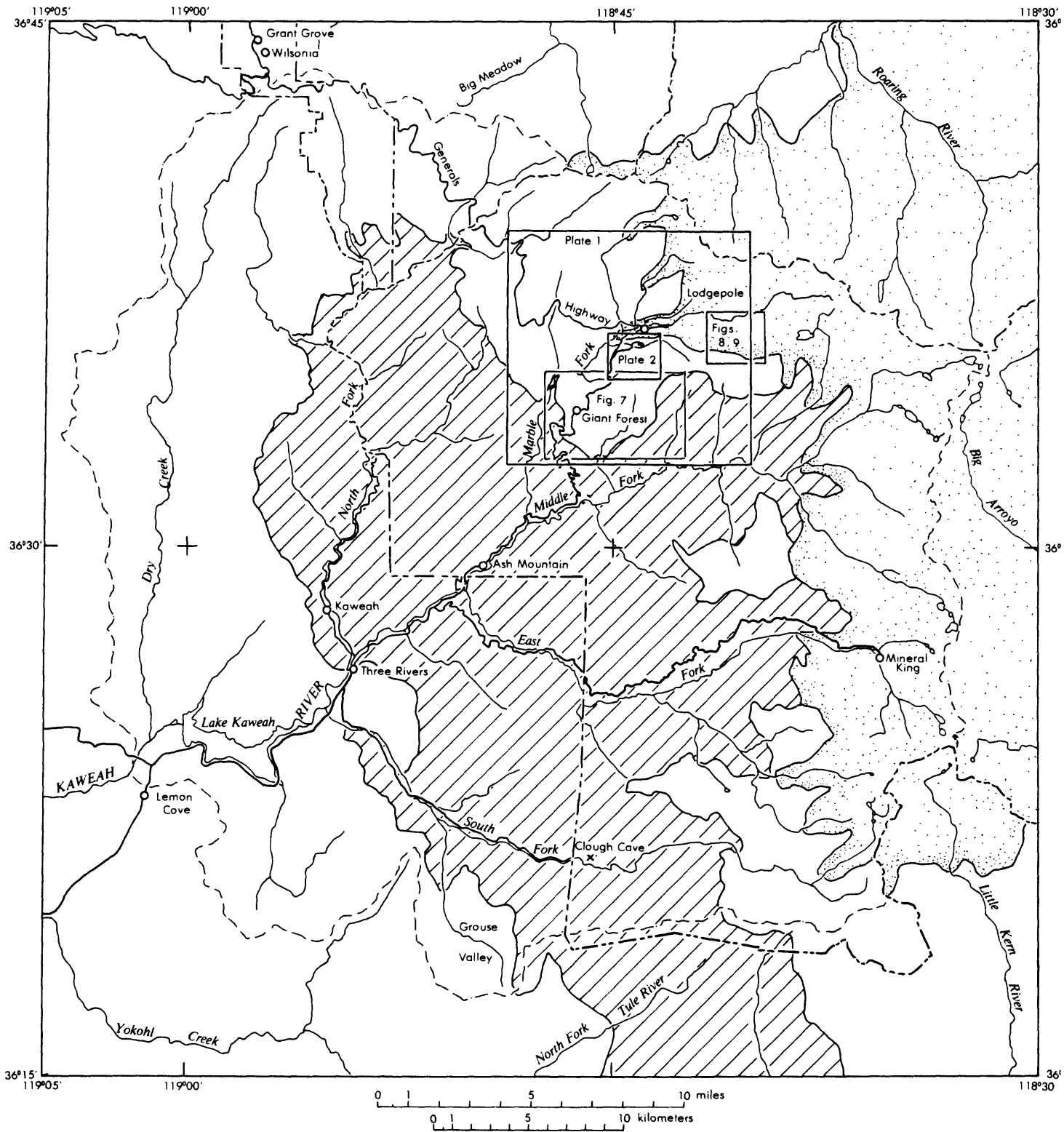


Figure 1. Map of the western part of Sequoia National Park and vicinity, showing locations of Plates 1 and 2 and of Figures 7, 8, and 9, and the area of the three topographic types described in the text. Diagonally lined area, type 1 (high steep straight slopes); blank area, type 2 (stepped topography); stippled area, type 3 (glaciated mountainland). Thin dot-dash line, drainage divide around the drainage basin of the Kaweah River; heavy line with two short dashes, park boundaries; heavy solid lines, major roads. Base from U. S. Geological Survey 1:125,000-scale map of Sequoia and Kings Canyon National Parks and vicinity, California.

Geomorphology of the Kaweah Basin, Sequoia National Park

The ground-water basins at Wolverton and beneath Crescent Meadow in Sequoia National Park are in alluvium in shallow valleys of the plateau area of Giant Forest. The alluvium beneath the Wolverton area accumulated behind a morainal dam and is over 100 feet thick in places. No glacial deposits or landforms are present near Crescent Meadow, and the alluvium there is very shallow.

While it is not necessary to understand the history of these sites in order to measure the volume of the ground-water reservoirs beneath them, provided enough drill hole and seismic data are obtained at each site, an understanding of their origin makes possible extrapolation from a relatively small number of data to consideration of the movement and storage of water beneath these and other meadow areas of the Giant Forest plateau. Our knowledge of this history is still very imperfect, as the following paragraphs show. But what is known and what can be reasonably inferred are presented below.

The usual picture of the origin of the present Sierra Nevada¹ is that it is the emergent part of a tilted fault block of crystalline—mainly granitic—rocks, uplifted along its east side along a system of faults, and tilted westward toward the Great Valley, which is the down-tilted part of the fault block, buried beneath alluvium. This history was developed mainly in the northern Sierra Nevada, between Yosemite and Lassen Parks, where stream gravels within a superjacent cover of essentially undeformed Cenozoic volcanic and sedimentary rocks, preserved on interfluves between the major west-flowing streams, provide the evidence on which that history is based (Lindgren, 1911; Matthes, 1930; for a review, see Bateman and Wahrhaftig, 1966, p. 129—169).

The topography of the Sequoia Park region does not fit well into this simple picture. It is true that the east-facing fault scarp that makes the high, steep, and narrow eastern slope of the Sierra Nevada is much better developed here than is the diffuse fault system farther north. However, the western side of the range is not one continuous west-sloping declivity of 75 to 150 feet per mile as it is farther north. The range at the latitude of Sequoia Park has a double crest, and the Great Western Divide, its western crest, is almost as high as the main drainage divide along the top of the east-facing fault scarp facing Owens Valley, and lies 8 to 20 miles west of the main crest, with the south-flowing Kern River between. The presence of this second crest 10,000—13,000 feet high, only 25—30 miles east of the Great Valley at 500 feet altitude, means that the western slope is in general much steeper than it is farther north and has elements as precipitous as the eastern slope.

Farther north, rivers flow west and southwest on courses presumably consequent on the westward slope of the range. The tributaries of the Kaweah, however, have a remarkably palmate pattern. The five main forks come together from different directions, and the North Fork in places flows southeasterly toward the higher parts of the range. No sign of faulting is present in the bedrock or topography to account for this apparently anomalous stream pattern, so it must be assumed that the river and its major tributaries acquired their pattern before uplift and tilting, and have maintained that pattern as they cut their canyons. Once they incised their canyons to depths of 1,000 feet, a major disruption of the landscape would have been required to pond the streams and cause them to overspill their divides and take different courses; and apparently

¹As used here, the term granitic rocks includes granite, quartz-monzonite, granodiorite, and diorite.

tilting proceeded slowly enough, and down-cutting rapidly enough, that such ponding never occurred.

Three strikingly different kinds of topography make up the Kaweah Basin in the Sierra Nevada (Figure 1). The first type, common in many mountain ranges but less so in the Sierra Nevada, covers a large central area of the basin, stretching northerly across all five sub-basins. It makes the steep transition from high mountain-lands to low foothills, and consists of relatively straight slopes several thousand feet high at inclinations of 22° to 39° , which are intricately dissected by ravines spaced 300–1,000 feet apart. This is the topography generally found in rugged mountain-lands where bedrock is mantled in large part by a layer of soil and rock debris that has weathered in place or accumulated by isolated rockfalls. Small patches of such soil and debris are mobilized on the rare occasions of extremely heavy precipitation and ground saturation into debris avalanches which may be accompanied by massive rockfalls. These commonly run down the slopes or steep ravines directly into the stream beds, and their detritus is carried on downstream during major floods. The bulk of the erosion of these steeply sloping mountain-lands is the integrated effect of these infrequent debris avalanches, that occur whenever the effects of weathering or rockfall accumulation create a mantle thick enough to become unstable during heavy rains. The origin of this topography will not be discussed further, because the areas of concern in this report do not lie within it.

The second topographic type consists of rolling plateaus and broad benches decorated with dome-like mountains and occasional rugged knobs and spires. The plateaus and benches occur at many different levels and descend from one to another by irregular steep bluffs with numerous outcrops and cliffs. Streams in this topography have quiet sandy reaches across the plateaus, and descend the bluffs via cascades and waterfalls. Thus their longitudinal profiles are irregular, unlike the profiles of streams in the first topographic type. This topography has been called a stepped topography (Wahrhaftig, 1965, see also Bateman and Wahrhaftig, 1966, p. 149-155).

This kind of topography occurs in two parts of the Kaweah drainage:

- (1) in the foothills below and west of the steep slopes of the first topographic type—for example, south of Lake Kaweah and around Grouse Valley; and
- (2) above the region of steep slopes, where it makes the plateaus of Giant Forest and at the head of the South Fork, and along the Generals' Highway between Lodgepole and the Kings River Canyon. The boundary of these plateaus with the region of steep slopes (the first topographic type) is usually a line of granitic outcrops and cliffs. This stepped topography occurs mainly on granitic rocks, and its probable origin is discussed below.

To the east of this upland plateau belt, and mainly in the headwaters of the Kaweah basin, is the third topographic type: a largely bare-rock region of sharp-crested peaks and ridges, U-shaped valleys, bowl-shaped valley heads (cirques), and many lakes. This topography is the product of glacial erosion during the Pleistocene, and is widespread throughout the High Sierra. Its origin is discussed in the section on Glacial Geology.

The Wolverton area lies on the boundary between the glaciated area and the stepped topography, and the Crescent Meadow area lies on the stepped topography of Giant Forest, just upstream from its contact with the first topographic type.

The Stepped Topography

The peculiar character of the stepped topography appears to depend on the weathering characteristics of granitic rocks, particularly those rocks that contain the mica biotite (Wahrhaftig, 1965). These characteristics involve, first, the hard and resistant nature of the unweathered rock; second, the way in which the rock is broken by joints¹; and third, the conditions under which granitic rocks weather and the nature of their weathering products, which are usually sand and clay and rarely anything coarser. Each of these characteristics is considered below.

Granitic rocks consist of aggregates of tightly interlocking crystals of quartz, feldspars, micas, hornblende, and augite. The individual crystals rarely exceed a centimeter in length, and are generally only a few millimeters across, but some crystals in the rock (called phenocrysts or megacrysts) may range in size up to 3 or more cm across. All the minerals except mica have hardnesses in excess of 5. Unweathered, these rocks are extremely resistant to abrasion or disintegration.

The granitic rocks are commonly broken into roughly rectangular blocks one to ten feet on a side by joint systems of at least three ages and modes of origin. The earliest systems formed soon after the consolidation of the granitic rock, and the joints of these systems contain dikes of pegmatite, aplite, or fine-grained diorite, or are coated with hydrothermal minerals such as epidote, chlorite, tourmaline, or quartz. In other parts of the Sierra Nevada, the commonest of these joints are spaced tens to hundreds of feet apart and dip northerly or northeasterly at angles of ten to thirty degrees. I did not observe them in the Wolverton area, but I did not look for them.

The second class of joints includes nearly vertical joints usually in two sets at nearly right angles, spaced one to ten or more feet apart. The sets may trend northeast and northwest or northerly and easterly. The orientation of sets of these joints may change abruptly across master joints (with more variable direction) spaced a mile or more apart. These joints appear to have formed in response to tension or torsion in the earth's crust; most of them appear to be pure tension cracks (Segall and Pollard, 1983a and 1983b). Later, in the Sierra Nevada, a small amount of shear (or fault displacement) took place along some of these faults (Lockwood and Moore, 1979). Usually this was a left-lateral strike-slip displacement of a few cm to a few meters on each fault.

The third and youngest kind of joint is parallel to the nearest land surface and is spaced 2 to 10 feet apart, usually becoming more widely spaced downward from the surface (Jahns, 1943). These last joints are attributed to the effect of removal of lithostatic load from granitic rocks that originally crystallized at depths of a few kilometers, where overburden pressures are equal to a kilobar (roughly 1,000 times atmospheric pressure) or more. These joints are called unloading joints, sheeting, or sheet structure. The term unloading joints will be used here. They were first described in the Sierra Nevada by G. K. Gilbert (1904) whose observations and inferences of origin have not been improved on.

The exact mechanism that forms these joints, which are pure tensional joints, is in dispute. That they form at or near the surface, and result in the expansion of the rock toward the surface, there can be no doubt, because they strike parallel to the walls of

¹ Joints are parallel planar fractures spaced at crudely regular intervals; all the joints parallel to each other are grouped into a joint set; and the rock may contain 3 to 6 joint sets. Two or more joint sets related in origin make a joint system.

valleys and canyons, regardless of the direction of the valley or canyon, and dip slightly less steeply toward the valley axis than the valley walls. They are behind most near-vertical cliffs in granite, such as the walls of Yosemite Valley. They are gently and broadly curved beneath the crests of hills and ridges, conforming closely to the land surface. It is unlikely that they extend very deeply into the ground, for intersecting sets of these joints are rare or non-existent, even where the topography has changed its shape drastically as it evolved—for example, in glacial cirques quarried into the sides of otherwise smoothly rounded mountains (see the observations of Gilbert, 1904, regarding this).

Evidence in the Wolverton area that these joints are mainly confined to shallow depths is contained in the record of drilling of holes W-9 and W-10 (Plate 2). There, frequent dropping of the drill bit through voids in the uppermost 30 feet indicated the presence of these joints beneath the dome-like ridge west of Long Meadow. From 30 feet to the bottom of the hole at 160 feet, apparently no joint sufficiently open either to cause the bit to drop or to carry and transmit water was encountered (Akers, 1984).

It is these last joints that control the development of topography in granitic rocks, for they provide planes of weakness along which the rock will slide or can be quarried, and are important avenues whereby water and atmospheric gases enter the rock and weather it. Thus once they are established, they tend to preserve the shape of the land-surface they are on, even though the erosional processes involved would be expected to give the topography a different shape. For example, the Grand Canyon of the Tuolumne in Yosemite National Park was filled to the brim with the largest, thickest, and probably most active glacier in the Sierra Nevada, yet still has a V-shaped cross-profile.

Because they form smooth, dome-like curves under the crests of hills and ridges, even though those crests may initially have been sharp and narrow, their continued peeling off tends to make the hills and ridges broadly rounded, and they lead to the formation of the "bald rock" or dome outcrops of granite so common in Sequoia Park and elsewhere in the Sierra Nevada. The mountain between Long Meadow and the General Sherman Tree is an example of this broadly rounded topography, developed on unloading joints.

The third factor responsible for the stepped topography is the chemical weathering of granitic rocks and the conditions that promote chemical weathering. Chemical weathering requires the presence of water and atmospheric gases, and is promoted by the presence of organic decay products, which make soil waters acid. In humid tropical environments all the mineral constituents of these rocks except quartz and similarly resistant minerals (*e. g.*, zircon, tourmaline) are ultimately weathered to clay minerals and ferric and aluminum oxides and hydroxides. In the temperate and rather dry climate of the Sierra Nevada, weathering of granite rarely goes this far. Instead, the granite weathers to coarse granite sand (called *gruss*) whose individual grains are commonly polymineralic aggregates of quartz, feldspar, etc. Microscopic study of weathering sequences in the Sierra Nevada show that the first mineral to show signs of weathering is biotite, which loses some of its iron by leaching and oxidation; about 1%–2% of the biotite is altered to the clay minerals montmorillonite and vermiculite, which expand in the presence of water (Wahrhaftig, 1965). The slight expansion that results shatters the surrounding rock; the cracks usually radiate from the biotite grains and follow cleavage directions in feldspar and amphibole (hornblende) rather than grain boundaries, to give rise to the coarse sand whose grains are composed of two or more minerals.

Since weathering requires water and atmospheric gases, and the fresh unweathered rock lacks porosity or permeability, weathering takes place initially along joint surfaces, and works inward to the centers of the joint blocks grain by grain as the weathering of each layer of grains provides tiny fractures leading farther into the rock. Weathering proceeds fastest at corners and edges where the rock is attacked from two or three sides; at any stage in the weathering of a joint block, the block probably consists of a rounded core of hard unweathered rock surrounded by a shell of rock more or less completely altered to gruss. The boundary between weathered and unweathered rock is commonly quite sharp. If the weathering process is interrupted by erosion before the blocks are completely reduced to sand, the cores may be exposed as rounded rock knobs or may litter the surface as boulders of weathering, called corestones. Many of the rounded granitic boulders in the beds of small streams may have acquired their form before erosion by this weathering process, rather than by being bounced along the stream bed.

The unloading joints are particularly likely avenues of penetration by water and of weathering attack, especially where there has been some expansion and arching of the slab above the joint. It is not uncommon to see three or four feet of crumbly gruss at the back of caves and overhangs along the exposed edges of unloading joints, with a strong weathering-induced "schistosity" of fine fractures parallel to the joint.

In the dry climate—with seasonal precipitation—of the Sierra Nevada, the soil may be moist for most of the year, but the impervious surfaces of rock outcrops dry out rapidly after each rain. Hence the proportion of the year in contact with weathering agents (particularly water) and, other things being equal, the rate of weathering per year, is far greater for rock buried beneath soil or its own weathering products (or covered with a mat of vegetation) than for rock exposed to the air as granite outcrops such as Moro Rock. Hence exposure converts granite in these climates from some of the most easily eroded rock—because it weathers readily to materials that can be easily eroded—to some of the most erosionally resistant rock, because then it weathers slowly and cannot be transported until it is weathered.

The gruss formed by weathering in the Sierra Nevada is easily eroded, even by surface runoff of heavy storms, and extreme gullying is prevented only by the fact that the surface soil, reworked by the biota, is highly permeable and porous and absorbs most rainfall. However, such sand, in transport by streams, does very little erosion of bedrock, except to polish the rock over which it flows. A stream needs gravel—pebbles, cobbles, and boulders—as tools to erode hard bedrock such as granite, and the temperate or tropical weathering of granitic rocks provides very little in the way of such tools. What few gravels there are come from pegmatite and aplite dikes and leucogranite that contain no mica, from mafic inclusions lacking biotite, and from rare bodies of metamorphic or volcanic rocks in the drainage basins.

The maximum depth of weathering is the depth at which water, as it seeps downward into the ground beneath the water table, loses its dissolved constituents (gases and acid radicals) that make it reactive with silicate minerals, and becomes saturated with soluble weathering products from the rocks. In this condition it is in equilibrium with the surrounding rock, and no more weathering takes place. Since the movement of ground-water through fractures in the rock decreases rapidly with depth beneath the ground-water table, the deeper water is likely to be saturated and unreactive. Hence there is a zone of maximum potential weathering of granitic rocks whose top is a foot or so beneath the ground surface and whose base is a few feet or tens of feet below the

ground-water table. Rock within that zone in contact with moist soil or gruss will weather. At or very close to the ground surface—above that zone—it weathers very slowly, and below that zone it weathers not at all.

In consequence of this regime of weathering, if granitic rock becomes exposed to the air along ridgecrests and away from streams, it ceases to weather and erode, but is surrounded by buried rock that continues to weather and to be eroded to lower levels. The exposure grows by differential lowering of the country around it into a rock monument, which will be a hill littered with corestones or a castellated crag—called in South Africa, a castle koppie—if the vertical orthogonal joints have controlled weathering. But it will become a dome or a bald rock if the unloading joints controlled weathering. In the Mojave Desert, hills initially mantled by corestones ultimately became smooth domes as the corestone mantle slowly disintegrated and unloading joints came to dominate the rock (Oberlander, 1972).

If the first exposures are in stream beds, as will probably be the case if base level is lowered or the land is uplifted or tilted and the streams rejuvenated, then the stream courses turn into a series of cascades or falls over the exposed bedrock, alternating with sandy graded reaches wherever the depth of weathering had exceeded incision. Although the streams can initially migrate off the bedrock exposures by cutting into gruss in their banks, ultimately each stream will be caught in a notch bordered by hard bedrock, and from that time on its basin upstream can be lowered to the level of the notch but not below, while the basin downstream from the notch can be lowered to the top of the next notch downstream (Figure 2). The lines of notches (with cascades) and rock outcrops grow, through differential lowering of the landscape controlled by these notches and outcrops, into the crests of bluffs that separate sandy plateaus and valleys. The stream with the lowest notch crossing any particular bluff can capture the headwaters of the other streams crossing that bluff, leaving their notches and the lines of intervening bluff-top exposures as a high rim bordering the plateaus upstream from the notch. A sequence of such plateaus and bluffs is a stepped topography. This is the kind of topography that dominates those parts of the west slope of the Sierra Nevada that have been developed on granitic rocks. Generally the step fronts, irregular in height and ground plan, face the Great Valley, and the tops of the steps slope gently back toward the higher parts of the Sierra Nevada, at least near their rims. Parts of the Giant Forest plateau are examples, as are Big Meadow in the Sierra National Forest between Sequoia and Kings Canyon National Parks and the plateau east of Clough Cave.

Steps also border the canyons of the major rivers (Bateman and Wahrhaftig, 1966). They occur on both sides of the southwest-flowing San Joaquin between Balloon Dome and Kirchoff Reservoir, and those on the west side of the river face east. They line the canyons of the Kern River and its tributaries; Chagoopa Plateau is probably such a step, and there are many steps in the Bartolas Country and the Domeland Wilderness.

The major rivers in the Sierra Nevada, which probably had enough metamorphic and volcanic rock in their basins to give them adequate cutting tools; and streams draining the higher parts of the range where glaciation and periglacial activity also provided abundant cobbles, pebbles, and boulders, were able to saw their way through the hard bedrock and establish relatively smooth longitudinal profiles in deep canyons. Nevertheless, they steepen abruptly at their headwaters where they are too small to have obtained much coarse material. Their deep canyons, incised into the stepped western front of the Sierra Nevada, control the development of smaller steps on their canyon walls. The major tributaries of the Kaweah seem to have developed such canyons.

Geomorphic evolution of the Kaweah Drainage in the light of Stepped Topography

The Sierra Nevada near Sequoia Park seems to have had a more complicated regime of uplift than farther north. A belt about 20 miles wide, between the eastern boundary fault and the Great Western Divide, appears to have been uplifted without tilting, except perhaps slightly to the south. The Kern River may have developed its south-flowing course on this tilt, and eroded its canyon along the zone of crushed rocks along the Kern Canyon Fault, which was last active tens of millions of years ago (J. G. Moore, oral comm., 1984). West of the Great Western Divide the shape of the uplift included a steep west-facing monocline, with a slope of about 400 feet per mile (4.3°), into which the forks of the Kaweah incised their steep-walled canyons. Rockfalls and debris avalanches probably kept a stepped topography from developing on these steep canyon walls, but a stepped topography did develop on the upper reaches of some of the forks, where there were no tools available for the streams to saw through the bedrock nickpoints exposed during down-cutting. West of the steep monocline the westward gradient of the tilted block flattened to about the gradients of tilting along the Kings and San Joaquin Rivers farther north. In this western foothill region of more gradual uplift, weathering processes had time to develop a mature stepped topography on the granitic rocks. The courses of the North Fork of the Kaweah and of Dry Creek are not well explained by this inferred history.

The barricade of granite outcrops along the rim of the Giant Forest plateau, represented by Moro and Beetle Rocks, enabled a complicated stepped topography with several minor levels of graded step tops to develop on the ridge west of Panther Peak (Figure 7). Crescent and Log Meadows are on one of these graded steps. Others are Circle Meadow, the bench around the General Sherman Tree, and Round Meadow just west of Giant Forest Lodge. A few much higher steps are on the west slope of Panther Peak, including Red Fir Meadow and a meadow above the south end of Log Meadow (Plate 2). The domed hills and ridges on this plateau include the ridge west of Long Meadow

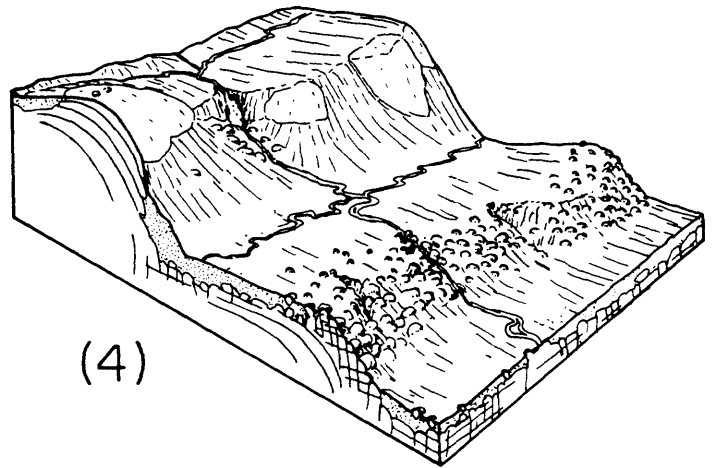
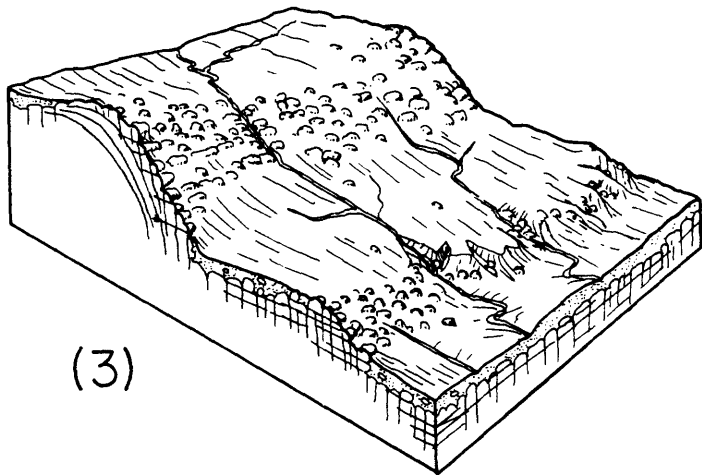
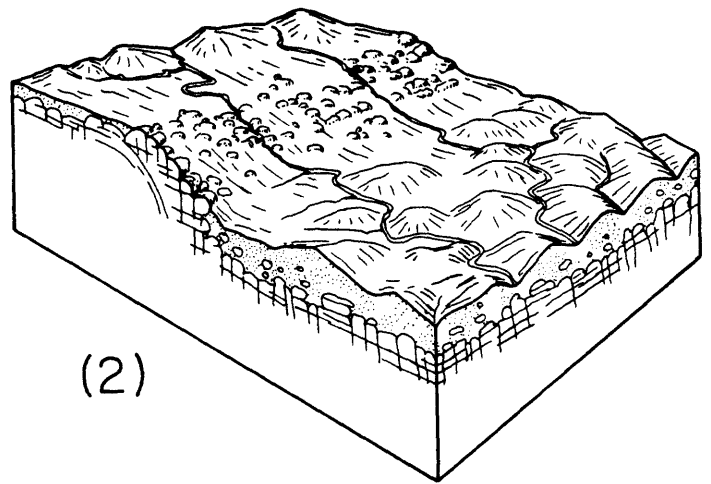
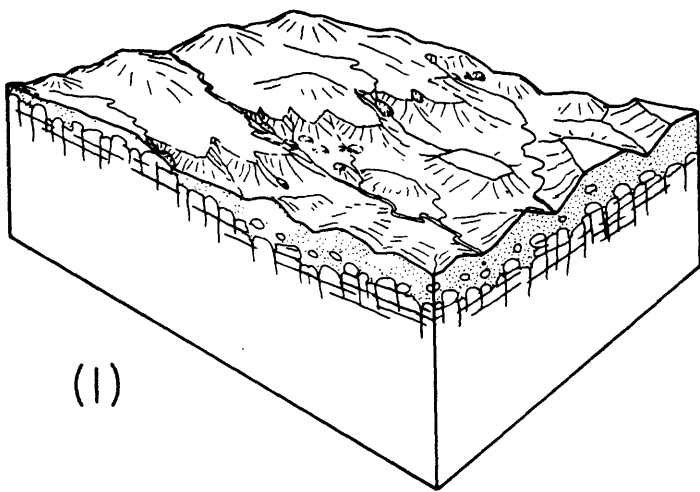


Figure 2. Stages in the Development of Stepped Topography. (1) Uplift or tilting causes streams to incise their beds into the gruss mantle of a deeply weathered granitic terrane; the streams encounter unweathered rock at places along their courses, and outcrops appear on hillsides. (2) Outcrops in stream beds act as local base-levels for erosion upstream, while the country downstream lowers as it weathers. (3) Outcrops appear in stream beds downstream, creating base-levels for the formation of a lower step; on the first step, one stream has captured the headwaters of another with a higher outcrop-controlled nickpoint, and rounded unloading joints develop beneath the step front. (4) Drainage has been reorganized by stream capture on the lower step; "bald rock" outcrops emerge on the front of the first step as the corestone outcrops are removed by erosion. If tilting rather than pure uplift caused the rejuvenation of the streams, the steps could develop simultaneously rather than sequentially. This was probably the case in the Sierra Nevada.

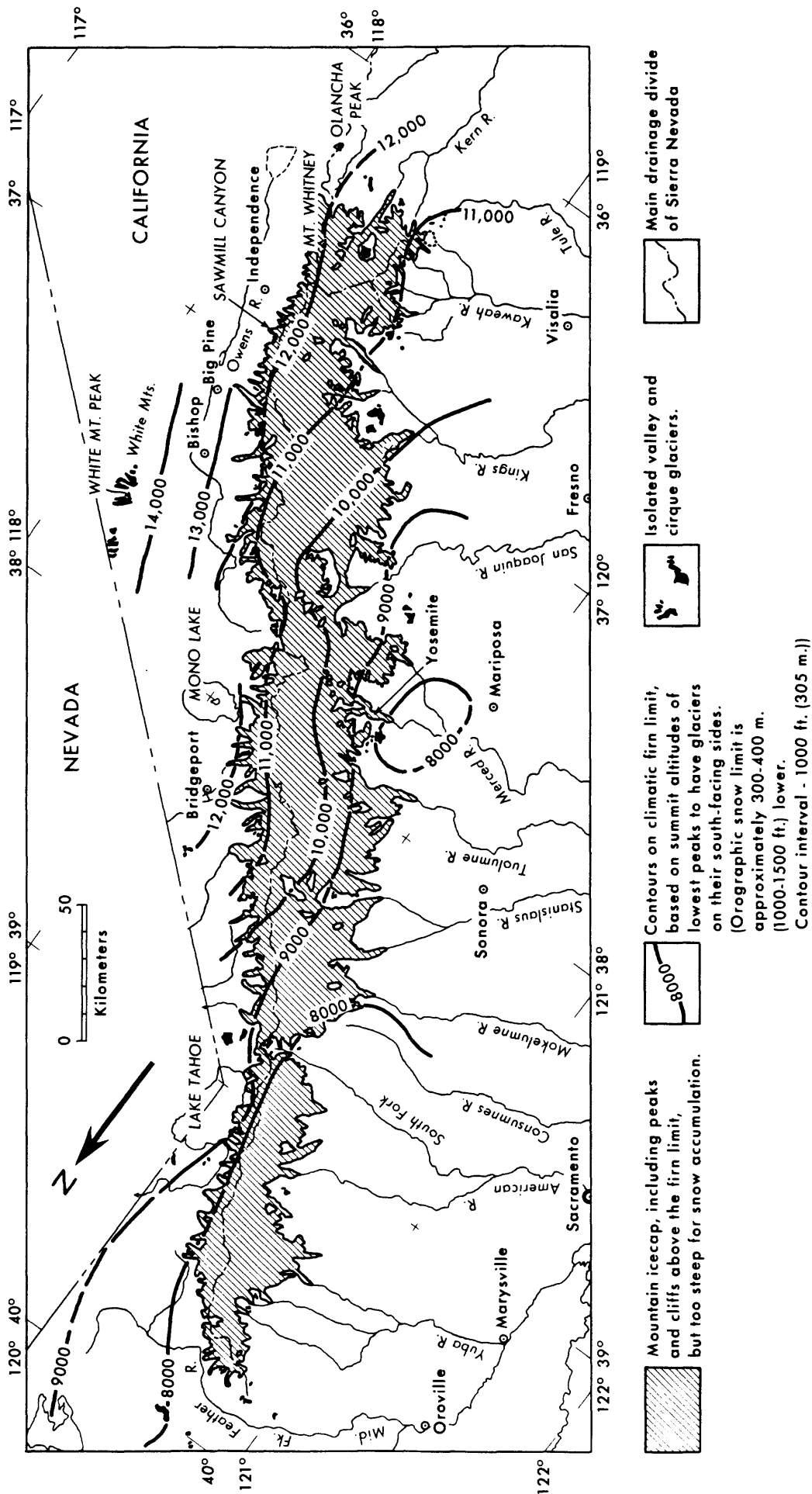


Figure 3. The mountain icecap in the Sierra Nevada and neighboring valley and cirque glaciers at the height of the Tahoe glaciation. The Kaweah and Kern River areas are at the extreme right (the south end of the icecap). From Wahrhaftig and Birman, 1965, figure 2.

Glacial Geology

The headwaters of the Marble, Middle, and East Forks of the Kaweah River and the upper Kern River drainage contain some of the most spectacular glacial topography in the United States. This glaciated region of Sequoia Park is the extreme south end of the mountain ice-cap that occupied the higher parts of the Sierra Nevada during parts of the Pleistocene Epoch (Figure 3). The alluvial ground-water reservoir of Wolverton and Long Meadow accumulated in a valley dammed by lateral moraines of the Marble Fork glacier, and ice appears to have extended down the Marble Fork to about the 5,900-foot altitude.

Glaciers

Glaciers accumulate wherever some of the snow that falls each winter persists through the following summer into the next winter's accumulation season. If this condition persists for a few centuries, the accumulating snow forms a deposit 100 feet or more thick, and the snow in the lower part of the deposit has been compacted, largely through sublimation and melting with re-freezing, into ice in which there are few if any interconnected voids. At a thickness of about 100 feet, the ice begins to flow outward under its own weight, and will begin to flow downhill on slopes at lesser thicknesses. The mechanisms of glacier growth and flow are described by Paterson (1969).

As the ice flows downhill, it enters regions of warmer climate, where the snow does not persist from year to year. The boundary where this occurs (*i. e.*, where accumulation from snowfall and avalanches minus melting and evaporation equals zero) is called the equilibrium line or firn limit. This is not a precise boundary, because of the vagaries of climate, but rather a zone over which this limit fluctuates from year to year. It is difficult to locate, even on existing glaciers, because its determination would require gathering data each year on the autumn day just before the next winter's permanent snow fell. It is even more difficult to determine on glaciers that no longer exist, and is usually reconstructed from the cirques of the smallest glaciers that can themselves be reconstructed. For example, the presence of glacial lakes such as Jennie and Weaver Lakes in the vicinity of Shell Mountain places the firn limit of the Tahoe through Tioga glaciations on north-facing slopes there at about 9,300 ± 100 feet.

The firn limit can be as much as 1,000 feet lower on the shaded poleward sides of mountains than on their equatorward sides exposed to the sun. The former firn limit we call the orographic firn limit, and the latter the climatic firn limit. For example, the orographic firn limit of the Tahoe and Tioga glaciations on the Alta Peak-Panther Peak ridge (Plate 1) was about 9,800 feet (given by the cirque in the middle of Sec. 26, T. 15 S., R. 30 E.), and the climatic firn limit was between 10,800 and 11,000 feet (given by the south-facing cirque one mile east of Alta Peak).

The section of the glacier through which the maximum amount of ice flows (*i. e.*, that has the maximum ice discharge) coincides with the firn limit, for as the glacier flows down-valley toward the firn limit, it is continually augmented by new net snowfall, and down-valley from the firn limit, more ice is lost by melting and evaporation (together called ablation) than is added by snowfall. As the glacier flows down-valley from the firn limit, more and more of the ice ablates, and the glacier grows thinner or narrower (or both). Ultimately a point is reached where the ice front can advance no farther, for the ice disappears there as rapidly by ablation as it is provided by inflow

from upstream. If the yearly rates of accumulation and ablation were constant, this point would be fixed. However, they are variable, and for that reason alone the terminus of the glacier is not likely to be fixed in position.

Glaciers flow at a rate (usually) of 30 to 600 feet per year (Paterson, 1969, p. 74). Thus, it would take ice from the head of the accumulation area east of Tokopah Valley, moving at a rate of 200 feet per year, about 200 years to reach its terminus 8 miles away. Consequently, it is possible for conditions at the terminus of a glacier to be quite out of phase with conditions at its accumulation area. But the response at the terminus, particularly to increases in the rate of snow accumulation, is faster than this velocity calculation would indicate, because the rate of flow of ice is very sensitive to increases in the thickness and to the slope of the upper surface; what is known as a "velocity wave" or "kinematic wave" resulting from the increase in snow supply, travels down the glacier at several times the rate of flow of the ice itself, and may produce an advance of the glacier terminus.

Glacial erosion

The ice velocity at the surface of the glacier is about half due to deformation within the ice, and about half due to slippage of the glacier over its bed. In other words, the glacier slips over its bed at about half the ice velocity measured on its upper surface. It is this slippage over the bed that is responsible for glacial erosion. As rock fragments embedded in the basal ice are dragged across the bedrock surface, they abrade the rock, cutting scratches and grooves, rounding bedrock knobs, especially on their up-glacier sides, and widening and deepening valley bottoms to give the characteristic U-shaped profile of glacial valleys. Wherever basal flow is especially strong, or the rock is easily abraded, bedrock basins are carved, which later hold lakes. On the lee sides of bedrock projections into the ice are regions of low pressure where meltwater re-freezes in cracks in the rock, prying loose blocks of bedrock that are incorporated into the glacial ice and quarried away from their bedrock sources, leaving jagged surfaces on the down-glacier sides of these bedrock projections. Rock knobs with smoothly abraded up-glacier sides and jagged and quarried down-glacier sides are called roches moutonees (sheep rocks) and are valuable indicators of the direction of glacier flow.

Another feature of glacial erosion is the bowl-shaped theatre-like valley head called a cirque, caused by the fracturing of rock through freezing in cracks of water that trickles into the rock through the great crevasse (or bergschrand) that opens at the head of a glacier during the summer season as ice pulls away from the rock at its head. This frost-wedging action saps the base of the cliff at the head of the cirque and causes the headward retreat of the cliff.

The cliffs behind the cirques and above the glacier surface elsewhere are also sculptured by the freezing of water in cracks in the rock—the expansion of water when it freezes to ice breaks and wedges out blocks—and by the avalanching onto the glacier surface of the blocks so detached. The falling blocks knock loose any projecting rock in their paths, and chip away fragments as they bounce down the cliff face. The hollows created by the detachment of these blocks and by the erosion they cause on their fall collect and hold more moisture, from rain or melting snow, than do the projecting ribs between them; they thus retreat more rapidly by frost-wedging than do the ribs, and if the cliff-face was initially smooth, it would eventually become intricately sculptured, especially with deep gashes (called couloirs) extending directly down slope. The sharp change in character and direction of the detailed modelling of the walls of glaciated

valleys, from intricate and jagged downslope-directed sculpturing above, to smooth sculpturing elongated down-valley below, marks the edge of the former glacier and makes it possible to reconstruct the former surface of the mountain ice-cap.

As the cliffs on opposite sides of a ridge (or drainage divide) are quarried back by frost action, they eventually intersect to form a sharp jagged rock crest called an arete, with sharp peaks, called horns (as in the Matterhorn), where the ridges branch.

Glaciated canyons are relatively straight and have U-shaped cross-profiles, in contrast to the sinuous V-shaped canyons produced by normal stream erosion. One possible explanation for the tendency of glaciers to straighten former stream valleys and broaden their floors is as follows:- at the slow velocities of glacier ice, the fastest flow is on the insides of bends, where the ice surface is steepest. At the high velocities of running water, inertia throws the fastest current against the outside of a bend. Thus whereas a stream erodes the outsides of bends preferentially and makes its course more sinuous (or meandering), glacial erosion is most intense on the insides of bends, removing the overlapping spurs of the stream-eroded canyon, and leaving a wide, straight canyon floor in their place. Another factor leading to the U-shaped cross-profile of glacial valleys is the tendency for any flowing medium to carve for itself a channel with a flat floor and steep banks. This is also the characteristic cross-section of a stream channel, which occupies only the very bottom of a canyon, whereas usually a large part or all of a glaciated canyon was once the channel of the former glacier that carved it.

The erosional evidence of glaciation thus consists of

- (1) sharp-crested aretes and horns at the headwaters of glaciated river systems.
- (2) cirques and lake basins carved by the ice as it flowed away from the headwater ridges to lower levels (there is no other way we know that lake basins in granite bedrock could have formed, without faulting);
- (3) U-shaped valleys with abrupt steps, some with waterfalls, in their longitudinal profiles (however, such valleys can also be formed by the processes leading to stepped topography);
- (4) roches moutonees, and other forms of glacial rounding;
- (5) scratches (also called striae), grooves, and percussion marks made by coarse fragments dragged by the ice over the bedrock;
- (6) glacial polish, the highly reflective rock surfaces that at first glance seem to be reflecting because of a film of water on the rock, and that are produced by the abrasion and polishing of the rock by very fine material dragged over the rock by ice.

Glacial Deposits

The material deposited by glaciers is an unsorted mixture of boulders, sand, and clay deposited by ice and is called till. Till may be deposited by the glacier on its bed as it is actively flowing (in which case the till is very compact and may have a parting or schistosity due to the weight of the overlying ice when it was deposited), or it may be left behind as the ice melted away, usually beginning as an accumulation of rock debris on the ice surface (in which case it is loose and porous). Other depositional evidence of ice includes glacial erratics, large boulders consisting of rock-types different from the bedrock on which they rest but present in the source area of the glacier. The most characteristic glacial depositional features in the Sierra Nevada are lateral moraines, massive linear ridges of till that rest on the sides of the glaciated valley and that extend parallel to the valley axis. These usually define the maximum lateral extent of the glacier that deposited them. In their great height and in the sharpness of their crests, the moraines in the Sierra Nevada are quite unlike glacial moraines in most other parts of the world, especially unlike those in subarctic regions such as Alaska. They appear to

have been formed in part as talus accumulations along the steep sides of the glacier, derived from superglacial till along the glacier's sides that slid off the glacier surface onto the moraine; The talus apron thus faced the valley walls on either side of the glacier. When the glacier melted away, that part of the talus apron that had been against the ice collapsed to form the slope of the moraine that faces the center of the glaciated valley.

Commonly, lateral moraines bend around at their lower ends to form terminal moraines, ridges of till deposited at the terminus of a glacier, that have the map-pattern of a U open up-valley. Most of the terminal moraines on the west side of the Sierra Nevada have been breached or removed by the swift meltwater streams, and it is doubtful that they were even deposited in the steep narrow canyons of most of the west-flowing streams such as the Marble Fork of the Kaweah. The glaciers that debouched onto the lowlands along the east base of the Sierra Nevada, on the other hand, left massive terminal moraines, some of which enclose glacial lakes.

The lateral moraine at Wolverton, which blocks the north end of Long Meadow is possibly the most easily accessible lateral moraine on the west slope of the Sierra Nevada, and is an ideal place to study and demonstrate the characteristics of these moraines.

Normally the meltwater issuing from a glacier would deposit the excessive load of coarse gravel that the glacier supplies it and would aggrade its bed for many miles downstream, forming a gravel plain called an outwash plain. On the west side of the Sierra Nevada, however, the glacial meltwater streams were generally too steep downstream from the glacial termini to deposit this material, and they carried most of it into the Great Valley, where it now makes up the alluvial plain of the east half of the valley.

The Record of Pleistocene Glaciations

The record of glaciation in Sequoia National Park is very fragmentary. Only for the last two glaciations can we reconstruct the extent of the ice with any confidence. The deposits of the older glaciers are too poorly preserved and so fragmentary that it is generally not possible to distinguish the separate ice advances that may have deposited them. The glaciers grew and melted away in response to climatic changes of long duration that are probably world-wide, so a record of all the glaciations that affected Sequoia Park could be sought elsewhere. Figure 4 is a correlation chart showing some of the sequences elsewhere that contain the evidence for the glaciations that may have affected the Sierra Nevada. In reading Figure 4, one must keep in mind that the vertical axis of the correlation chart is the time axis, and that the time scale changes at 10,000 years and at 150,000 years. A correlation of glaciations in the Sierra Nevada with those in the Cascade Range and the Rocky Mountains is given by Birkeland and others (1971).

On the eastern slope of the Sierra Nevada, where faulting has uplifted and preserved remnants of the older glaciations, the glacial deposits are intercalated with volcanic rocks whose ages can be determined by the ^{40}K - ^{40}Ar method. The glacial advances that have been recognized on the east side of the Sierra Nevada are shown in the third column of Figure 4. The glaciations were originally named by Blackwelder (1931) with additions by Sharp and Birman (1963), Birkeland (1964), and Curry (1966, 1971). Those now regarded as of doubtful existence, or that are thought to be equivalent to other named glaciations in the Sierra Nevada, are enclosed in double parentheses.

The record on the east side of the Sierra Nevada shows about eight glaciations

within the last 3 million years. This number is a minimum, because this is the minimum number of glacial events necessary to account for the relationships with each other of glacial landforms and of deposits of till, outwash, and glacio-lacustrine sediments found to date on the east side of the Sierra Nevada and in Owens Valley, and for the relationships of these landforms and deposits to the dated volcanic rocks. A more complete record could be expected in a basin of deposition, where all the sediments are preserved and are deposited in layers, successively younger upward. Two such basins exist, flanking the Sierra Nevada. On the west side of the range, the glacial meltwaters carried their burden of sediment into the San Joaquin Valley, where it has been recognized as a series of sandy alluvial formations, which are interpreted as outwash deposits carried from the Sierran ice-cap. During the interglacial following each glaciation, the rivers (no longer overburdened with debris) trenched their outwash fans, the deposits were eroded in part into rolling hills, and soils developed on them. Near the hinge line at the east edge of the Great Valley there was no subsidence and there may actually have been slight uplift accompanying tilting. The outwash of younger glaciations was deposited in the broad shallow trenches cut into the heads of the outwash fans during the preceding interglacial. The outwash deposits are now preserved beneath several levels of terraces within these broad fan-head trenches.

Continued subsidence nearer the valley axis, together with the raising of base-level when the rising oceans flooded San Francisco Bay and the delta, prevented down-cutting and entrenchment of the lower ends of the fans during the interglacials. Thus the fan-head trenches shallowed downstream and came to an end at mid-fan. Downstream from the ends of the trenches, each younger outwash deposit spread out over the depositional surface of the preceding outwash. Thus the alluvium near the center of the valley is a sequence of layers of glacial outwash, with only interbedded soils formed on parts of the fans to mark the periods of non-deposition during interglacials. The record of these terraces and alluvial sequences has been most recently studied by Marchand and his co-workers (Marchand, 1977; Marchand and Allwardt, 1981; Harden, 1982) and is shown in the first column of Figure 4.

In the southwest corner of the Great Basin, about 100 miles southeast of Giant Forest, is Searles Lake, a dry lake underlain by a thick sequence of alternating muds, salts, and clays. These have been studied by George I. Smith and his co-workers, and interpreted climatically in a number of papers (Liddicoat, et al., 1980, Smith, 1976, 1979, in press; Smith et al., 1983; Smith and Street-Perrott, 1983). The results of these studies are shown in column 4 of Figure 4, and are discussed in the next paragraphs.

Glacial melt-water on the east side of the Sierra Nevada south of Yosemite Park flows into the Owens River, which would now discharge its water into Owens Lake except that it is now diverted into the Los Angeles Aquaduct. During glacial periods, when there was much more water flowing down the river than now, Owens Lake overflowed south into Indian Wells Valley, and ultimately into Searles Valley, where Searles Lake, now dry, appears to have filled to overflowing.

A complicated sequence of layers of salts interbedded with layers of mud underlies Searles Lake. This sequence has been penetrated by many bore-holes to depths of about 150 feet and by a single bore-hole to its bottom at 2275 feet below the surface, where it rests on 695 feet of alluvial gravel that is underlain by bedrock (Smith, et al., 1983). The fine-grained mud layers consist largely of calcium and magnesium carbonates (the minerals calcite, dolomite, and aragonite) which precipitated out of solution in the lake waters shortly after their arrival into the lake. These carbonates are only slightly soluble and therefore had to have been transported to the lake in rather voluminous quantities of essentially fresh water. These carbonate muds are dark green because of

their content of ferrous iron, and they were deposited under reducing conditions which imply a deep lake. Smith and his co-workers (Smith, 1976, 1979, in press; Smith and Street-Perrott, 1983) interpret these muds as evidence of high runoff from the Sierra Nevada and therefore of glacial climates.

The salt beds consist of coarse crystals of a number of highly soluble salts, mainly complexes of chlorides, sulfates, carbonates, bicarbonates, and borates, of potassium, sodium, calcium, and magnesium, some with water of crystallization. These salt beds could be precipitated only from concentrated brines and represent periods when Searles Lake was dry or nearly dry. The salts actually precipitated as the lake was drying and the water became saturated in these very soluble components, and a layer of salt therefore represents the final stage in the transition from a wet to a dry climate. The salt was sometimes buried by a thin layer of impervious mud washed onto the dry lake surface from surrounding uplands, and therefore did not dissolve during the next high lake stand. Where those muds are yellow or orange, because their iron was oxidized to the ferric state through exposure to the atmosphere, Smith and his co-workers interpret them as playa deposits which, along with salts, indicate dry interglacial periods. Their interpretation of the layers encountered in the core holes is given in column 4 of Table 4.

The age of the deposits in Searles Lake, and of the climatic events that produced them, can be determined as far back as about 35,000 years by the ^{14}C method, using organic material deposited in the muds. The entire core, however, spans a period of a few million years. To establish the ages of the older segments of the core, use is made of the fact that the earth's magnetic field has reversed itself at irregular and apparently random intervals throughout much of geologic time, with the north magnetic pole being near the north geographic pole during roughly half the time, and near the south geographic pole during the remainder. As described below, these reversals can be dated and are detected in the sediments deposited in the lakes and on the ocean floor.

The fact that the earth's magnetic field has reversed many times was determined through investigations combining measurements of the magnetic polarity of young volcanic rocks with radiometric dating of the same rocks. When volcanic rocks are erupted onto the surface, the tiny grains of magnetite and other magnetic minerals that crystallize out of the magma acquire a permanent magnetization induced by the earth's magnetic field as they cool through the Curie temperatures of the magnetic minerals (about 400° – 600° C). This is the same temperature range at which other minerals in the rock start retaining the ^{40}Ar produced by the radioactive decay of the ^{40}K they contain. By collecting samples of the rock whose orientation in the outcrop is marked and recorded before detachment, it is possible to measure in the laboratory this thermoremanent magnetic orientation and to determine easily whether the rock cooled when the earth's magnetic field was as it is today—that is, during a period of normal magnetic polarity—or during a time when the magnetic needle that now points north would have pointed south—that is, during a period of reversed magnetic polarity. (Whether a rock sample is magnetically normal or reversed can even be determined in the field, using a simple portable field magnetometer or a couple of geologist's brunton compasses.) The absolute age of the rock sample is determined by the ^{40}K - ^{40}Ar radiometric dating method. By determining the magnetic polarity of many young dated volcanic rocks, a paleomagnetic time scale has been determined back to about 5 million years (Mankinen and Dalrymple, 1979; see also Cox, 1973; Glen, 1982). The irreducible errors and uncertainties in the ^{40}K - ^{40}Ar dating of rocks older than about 5 my are equal to or greater than the duration of the individual magnetic polarity intervals; consequently older paleomagnetic polarity intervals cannot be determined by this method, but must be determined by other means. The currently accepted paleomagnetic reversal time scale for the last 3.5 million years (Harland and others, 1982, p. 66–73) is shown in column 5 of

Figure 4, and has been applied to the sediments of Searles Lake (Liddicoat and others, 1980).

The most complete record of glacial and interglacial cycles comes from the deep-sea piston cores from the world's oceans. It is interpreted as a record of the fluctuation in the volume of the oceans as water that evaporated from them was stored on land in the form of the continental ice sheets, but this record is in the form of the ratios of the oxygen isotopes ^{16}O and ^{18}O in the carbonate of the shells of one-celled marine organisms called foraminifera. The ratio of these oxygen isotopes varies for two reasons: (1) it is proportional to the oxygen isotope ratio in the sea-water in which the organisms live (a ratio that varies as the volume of water in the global ice sheets fluctuates); and (2) the ratio at which the isotopes from water of a given isotope composition are incorporated into the carbonate of the shells varies with the temperature of the water. Shackleton and Opdyke (1973), Berggren and others (1980), and Harland and others (1982, p. 41-44, 63-66) discuss the methodology and the resulting time scale. A composite record of the variations in the ^{18}O - ^{16}O ratio in foraminifera from deep-sea cores is shown in column 6 of Figure 4. Although both the oxygen isotope ratio of the sea-water and the water temperature have influenced this curve, their influence is in the same direction, and the variation in oxygen-isotope content of the water is by far the most important factor. The cause for this variation is explained in the next paragraph.

Water molecules (H_2O) with the formula H_2^{16}O (molecular weight, $m = 18$) are 10 percent lighter than water molecules with the formula H_2^{18}O ($m = 20$). Since, at a given temperature the kinetic energy of all molecules in a substance such as water averages the same (there is a distribution of kinetic energies around this average), the average velocity (v) of molecules of H_2^{16}O will be 5 percent higher than the average of the molecules of H_2^{18}O (Kinetic Energy = $mv^2/2$). Hence, at a given temperature, more of the light molecules would reach high enough velocities to escape by evaporation from the sea surface than would the heavy molecules, and the escaping water vapor would be richer in H_2^{16}O than the sea-water from which it came. This water slightly richer in ^{16}O provides most of the precipitation on land and on growing ice sheets. Thus, during a glaciation, sea-water becomes impoverished in ^{16}O and residually enriched in ^{18}O . When the ice melts, the ^{16}O is returned to the sea, and the concentration of ^{18}O decreases slightly. The ratios of the isotopes in the silica and lime secreted by the microorganisms are proportional to their ratios in the sea-water, and the record of these fluctuations is therefore preserved in the fossils contained in sediments that accumulated on the sea-floor.

This record can be calibrated to an absolute time scale (in thousands or millions of years) first, by the use of ^{14}C dates on the lime in the fossils in the uppermost parts of the cores (going back roughly 60,000 years). The older parts of the cores have to be dated by interpolation from known points in the paleomagnetic reversal time scale.

As in the sediments deposited in Searles Lake, the fine particles of magnetite settling through sea-water come to rest on the bottom preferentially aligned (as tiny magnets) parallel to the earth's magnetic field of the time. The piston cores are collected by driving a tube into the soft ooze of the sea-bottom in such a way that the core can be brought to the surface undisturbed. Through sensitive magnetometers, the direction of magnetization of thin slices of core can be determined. If the core was collected from a high latitude, the magnetic vector will be steep and it is possible to determine directly which parts of the core were deposited during magnetically normal periods (when the north-seeking direction would point downward in cores from high northern latitudes and upward in cores from high southern latitudes), as was done with the Searles Lake core, 36°N . In cores collected from equatorial regions, however, the

magnetic vector is horizontal (perpendicular to the core axis), and since we cannot know the orientation that the core had on the sea-floor, other than to know that it was vertical and which end was up, we cannot tell from the measurement of any single core sample whether it is normal or reversed. However, because the core is not internally disturbed, differences in direction are easily apparent, and it is found that the magnetization in equatorial cores is mainly in two horizontal directions antiparallel to each other. If the sediment less than 700,000 years old at the top of the core is preserved (which can be checked by ^{14}C dating on carbonate shells of foraminifera near the top of the core), then its magnetic direction must be the normal direction, and normal and reversed segments of core can be determined. The intervals of normal and reversed magnetic polarity are of widely differing lengths, ranging from a few tens of thousands to several hundred thousand or about a million years, and the pattern in the cores can be matched to the magnetic polarity time scale worked out on land through the K-Ar dating of volcanic rocks. The best deep-sea oxygen isotope records come from cores whose ages were determined through calibration with the paleomagnetic time scale in this way.

We know from studies elsewhere in the world that late Cenozoic glaciation began as far back as mid-Miocene (10-15 m. y. ago) in Antarctica and Alaska, and it began in Iceland about 3 million years ago. There is some evidence of glaciers in the Sierra Nevada as early as 3 million years ago (Curry, 1966; Figure 4, column 3) but that evidence has recently been called into question by Huber (1981). The record of the deep-sea cores described above shows over the last 900,000 years about eleven cold periods with extensive glaciation separated by warmer periods similar to the present, and about ten such additional glacial periods in the interval from 0.9 to 1.9 million years ago. Earlier than this the record is unclear, except that extensive accumulation of northern-hemisphere ice sheets seems to have occurred for the first time slightly after 3.2 million years ago (Shackleton and Opdyke, 1977). Thus, the great majority of the glacial episodes indicated in the deep-sea records either had no counterparts in the Sierra Nevada, or have left no landforms or deposits by which they can be sorted out. Presumably the carving of the cirques and glacial valleys and the building of some of the massive moraines in the Sierra Nevada were the work of many glaciations, but we have only a clear record of the last few.

Smith (in press) points out that the Searles Lake record differs in many significant respects from the record in the deep sea cores. In particular, the long period of high water from 3.2 to 2.5 million years ago, and the long period of dessication indicated by the playa and saline deposits of from 2.5 to 2.0 million years ago have no counterparts in the deep-sea record, which shows fluctuations with about a 100,000-year periodicity then as at other times in the Pleistocene. Also, although the deep sea record and the Searles Lake record are in phase for the last 100,000 years, they seem to have been out of phase frequently in the interval between 600,000 and 100,000 years ago, and especially at 130,000 years, when an abrupt rise in lake level coincided with an abrupt change from a glacial to a non-glacial climate world-wide. These differences in chronology may be because of subtle climatic cycles with a periodicity on the order of half a million years, as Smith suggests, or because of tectonic changes affecting the Owens River drainage into Searles Lake, as I suspect.

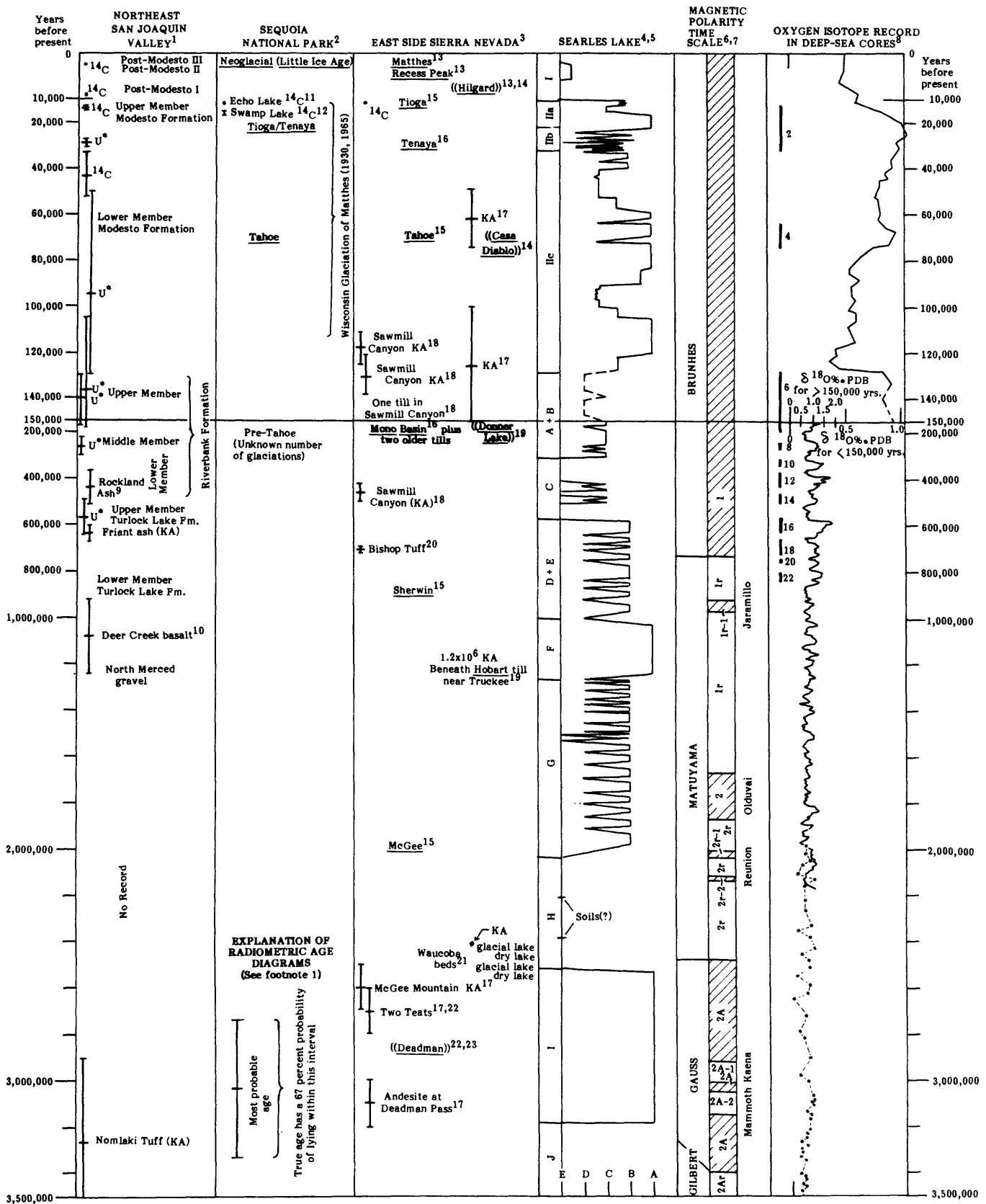


Figure 4. Correlation chart of climatic events and deposits in the Sierra Nevada, San Joaquin Valley, Searles Lake, and Deep Sea Cores.

Footnotes for Figure 4

1, Marchand and Allwardt, 1981; ^{14}C , Carbon-14 date; U^* , Uranium disequilibrium date; KA, Potassium-Argon date; FT, fission-track age; for explanation of symbols for preferred age and error bar see bottom of Column 2; for discussion of age of Friant ash see Sarna-Wojcicki et al., 1984; lower member of Turlock Lake Formation has reversed magnetic polarity (Packer et al., 1977). 2, Matthes, 1930 and 1965, Birman, 1962, and this study; ^{14}C dates are from Echo Lake near Lake Tahoe (Adam, in press) and Swamp Lake near Miguel Meadow in Yosemite National Park (Batchelder, 1980). 3, References are listed in footnotes below; underlined words are named glaciations; footnote following underlined name refers to article first naming the glaciation; see footnote 1 for meaning of radiometric dating symbols. 4, Smith, 1979, Fig. 41, for period 0-150,000 years; 5, Smith, et al., 1983, fig. 6, for period older than 150,000 years; for magnetic polarity, see Liddicoat, et al., 1980; Named lithologic units indicative of climatic episodes are indicated at sides of chart as follows: I, Overburden Mud and Upper Salt; IIa, Parting Mud; IIb, Lower Salt; IIc, Bottom Mud; A though I, members of the Mixed Layer; J, Alluvium; letter symbols at bottom of column define lake levels as indicated by extent of curve to the right, as follows:- A: lake deep, overflowing most of time; B: lake deep, slightly saline, overflowing only part of time; C: Lake shallow, moderately saline, overflowing rarely if at all; D: lake shallow to dry, very saline; E: lake a playa or salt flat most of year, flooded intermittently. 6, Harland et al., 1982; diagonal lining, normal magnetic polarity; blank, reversed magnetic polarity; words in capital letters on left are polarity chrons; words in lower-case letters on right of the bar time scale are polarity events; numerical designations within the bar scale are as defined in Harland et al., 1982, p.66-67; 7, Mankinen and Dalrymple, 1979. 8, ^{18}O percentage increases to right; hence glacial conditions are marked by right-hand peaks in curves; note that the scale for ^{18}O percentages changes at 150,000 years; period from 0 to 150,000 years, redrafted from Smith, in press, Fig. 3; period from 150,000 to 2,100,000 years redrafted from Berggren et al., 1980, Fig. 1, to fit the magnetic polarity time scale; period from 2,100,000 to 3,500,000 years from Shackleton and Opdyke, 1977, Fig. 2, redrafted to fit Berggren et al., 1980, Fig. 1, and the magnetic polarity time scale of Harland et al., 1982; numbers in left-hand column are marine isotope stages of Emiliani, 1955, 1966, and Shackleton and Opdyke, 1973, as quoted and referenced by Shackleton and Opdyke, 1976. Even-numbered stages, marked by black bars, are glacial. 9, Sarna-Wojcicki et al., in press; Meyer et al., 1980. 10, Harwood and Helley, 1981, and E. J. Helley and D. S. Harwood, written communication, 1984; 11, Adam, in press and oral communication, 1984; 12, Batchelder, 1980, see also Adam, in press; 13, Birman, 1964; 14, Curry, 1971; 15, Blackwelder, 1931; for estimate of age of the Tahoe, based on weathering rinds, see Colman and Pierce, 1981; 16, Sharp and Birman, 1963; 17, Bailey, et al., 1976; 18, Gillespie, 1982; 19, Birkeland, 1964; 20, Bailey et al., 1976; 21, Hay, 1964; G. H. Curtis, oral communication, 1977; 22, Curry, 1966; 23, Huber, 1981.

Glacial Geology of the Wolverton-Lodgepole Area

In the Wolverton-Lodgepole area only three ages of till were confidently distinguished in this investigation. They are:

(1) Youngest: Fresh unweathered till, which consists of an assemblage of fresh granitic boulders with loose porous interstitial gravel and sand, making sharp-crested moraines that have closely spaced or touching boulders on their upper surfaces. On Plate 1 this is shown as Tioga till.

(2) Intermediate: Massive moraines of till whose road-cut exposures show that many—and in places most—of the buried granodiorite boulders have disintegrated at least partly to gruss. The summits of these moraines tend to be rounded, and exposed boulders along their crests are generally a few meters apart. On Plate 1 this is shown as Tahoe till. The intermediate moraines indicate a more extensive glaciation than do the youngest moraines.

(3) Oldest: Outside the ice limits defined by the intermediate moraines, a few glacial erratics and patches of glacial till give evidence of at least one earlier ice advance more extensive than the glaciers that deposited the intermediate moraines. On Plate 1 this is shown as pre-Tahoe till.

The glacier that deposited the youngest till (Group 1) extended down the Marble Fork to just downstream of the 6,400-foot contour line. Its south limit was intersected by the General's Highway at the 6,800 foot contour line in the SE 1/4 of Sec 20, T. 15 S., R. 30 E., and its north limit is intersected by the highway about 500 feet west of Silliman Creek.

Till of the intermediate stage (Group 2) makes the massive moraine along the north side of Wolverton Creek, as well as the moraines south of Willow Meadow. Its glacier extended down the Marble Fork to about the 5,900-foot contour. The ice limits west of Silliman Creek and Wolverton Creek are obscure, and the till there is patchy.

Erratics of the oldest group (Group 3) are found along the General's Highway for about 1,000 feet south of Wolverton Creek, in places between Wolverton Creek and the Wolverton Road, and on the ridge between Silliman and Clover Creeks at about 7,200 feet altitude. The plateau around Willow Meadow may be underlain by till of this age. Patches of till of this age have been recognized by Moore and Sisson (See Plate 1) along Clover Creek. A patch of surficial material containing erratic boulders south of Wolverton Creek and just east of the lower end of Long Meadow may belong to this group. It is labelled "ancient till" on Plate 2.

The most extensive published study of the glacial geology of Sequoia Park is the summary of Francois E. Matthes' (1965) work, prepared posthumously by Fritiof Fryxell as U. S. Geological Survey Professional Paper 504-A. The work on which this paper was based was done by Matthes in the 1930's with one supplemental field season in 1952 by Fryxell. It uses the nomenclature for glaciations developed by Matthes (1930) in Yosemite Valley. There appears to be a misprint in the text (P A-28), for the downstream limit on the Marble Fork of both the Wisconsin (Matthes' youngest) stage and the El Portal Stage (his intermediate) are given as 5,350 feet. Judging from his map, Matthes' Wisconsin stage includes both the youngest and intermediate deposits of this report, and his El Portal Stage corresponds to the oldest deposits of this report. Although I feel confident that Fryxell recognized the difference between the youngest and intermediate deposits that I have reported, I am sure that he felt constrained by the responsibility of describing the geology as Matthes would have done it, not to mention this difference.

Birman (1962) divided the youngest till (Group 1) into till of the Tioga (youngest) and Tenaya (next youngest) glaciations. He assigned the till of Group 2 to the Tahoe glaciation. His criteria for distinguishing between the Tioga and Tenaya tills are based on the number of fresh and weathered boulders along selected reaches of the moraine crests. The classification (fresh or weathered) into which a boulder falls depends on the preservation of the glacially abraded surfaces, on the appearance of a weathered surface, and on the extent of patches of weathered rock on the outer surface of the boulder. I have found it difficult to apply Birman's criteria systematically, either here or in the Yosemite Park region, especially during a reconnaissance investigation. I have also difficulty with the conceptual model on which the distinction is based, inasmuch as boulders buried in till appear to weather much more rapidly than boulders that were never buried (for the reasons given in the discussion of stepped topography); hence different weathering ratios may be measured on moraines of the same age depending on the post-glacial erosional history of the moraine. The crude measure of relative age I have used—following Blackwelder (1931)—the distance between boulders along the crests of moraines, is not refined enough to pick up any difference between the Tioga and Tenaya moraines, as identified by Birman (1964), where I mapped them in Yosemite Park and vicinity, and the two are mapped here as one unit.

By determining the locations of a few boulder counts in Birman's (1962) Table 3 (p.7—17) I have determined that the outer limit of his Tenaya till corresponds to the outer limit of the Group 1 moraines mapped here, and that the Tioga glacier according to him had its terminus at about 6,600 feet on the Marble Fork, a short distance upstream from the mouth of Silliman Creek. I did not examine the boulders of any of his Tioga till on the Marble Fork so cannot say for certain how much it differs from his Tenaya till. Judging from my studies of moraines of similar position in Yosemite Park and vicinity, it is unlikely that the Tenaya ice was significantly older than the ice that deposited the Tioga moraines, and I prefer to regard both as having been deposited during a single glaciation, probably corresponding to the Wisconsinan of the mid-continent.

Birman and I are in agreement in assigning the till of Group 2 to the Tahoe glaciation. Jay Akers (written communication, 1984) reports that his hole W-12 (Plate 2), drilled on the southern edge of the moraine, near the northwest corner of the Wolverton parking lot, encountered a water-saturated mixture of material ranging from coarse sand to clay, having the appearance and consistency of plaster, from 6 feet to 70 feet below the surface. The hole bottomed at 70 feet without encountering any boulders. Thus it appears that the till beneath the Tahoe moraine has had all its pores plugged by the fine weathering detritus, and acts as an aquaclude, holding ground-water in the Wolverton-Long Meadow basin. Sand and gravel are common in the holes drilled into the alluvium of this basin and there is no indication that a lake ever occupied the basin. Thus alluviation must have been concomitant with the building of the morainal barrier.

The Tahoe till is much more weathered, both underground and at the surface, than the Tioga-Tenaya till. In a few localities elsewhere (most notably in a roadcut in the east moraine of Cascade Lake in the Tahoe basin of the northern Sierra Nevada) it is possible to see that this weathering took place before the deposition of the Tioga-Tenaya till, for there the fresh younger till (mapped as Tioga) rests on the weathered Tahoe. The impression that these exposures give is that the interval of time between Tahoe and Tenaya-Tioga times is much greater—possibly an order of magnitude greater—than the interval since the Tioga was deposited. If the end of the Tioga is 10,000 years ago, then the Tahoe should be 100,000 years old or older, and probably correlates with the Illinoian glaciation of the mid-continent, and should coincide with the penultimate glacial period identified in deep-sea cores, which reached its maximum approximately 150,000 years ago. This age is difficult to bring into agreement with the latest determination of the

age of basalt from beneath till identified as Tahoe at Sawmill Canyon near Big Pine of about 90,000 years ago (Gillespie, 1982, p. 189—380), or with the age of the Tahoe as determined from weathering rinds on andesite boulders in the northern Sierra Nevada (Colman and Pierce, 1981).

The oldest till and erratics of Group 3 are commonly more weathered and altered to gress than the Tahoe till. They are presumably residual boulders left after the removal of much of this older till by weathering and erosion, and presumably before the Tahoe till was deposited. This suggests that the older till, including the "ancient till" of Plate 2, is as much older than the Tahoe till as the Tahoe is older than the till of the Tenaya-Tioga group.

Volume of the Wolverton Ground-water Basin

The imperviousness of the till in hole no. 12, and the lack of springs along the north side of the Tahoe moraine north of Wolverton Creek, mean that the till barrier along the north side does not contribute significantly to the readily available ground-water of the Wolverton-Long Meadow area. Thus the ground-water basin is confined to the alluvium south of the moraine. Cross-sections of this basin (Figure 5) show the depth of the basin based on the seismic surveys by John Tinsley (see last section of this report) and the earlier seismic surveys reported by Bertoldi and Miller (1969). On these cross-sections are plotted the logs of the holes drilled under the supervision of Jay Akers in 1983 (written communications, 1983 and 1984) and the logs of the production and observation wells drilled in 1967 (Croft et al., 1968). The lines of the cross-sections are shown on Figure 6. Inspection of the well logs shows that roughly half of the alluvium is sand and gravel and half silt and clay.

Using the data from the seismic surveys, supplemented by depths of wells, a contour map was drawn of depth to basement (Figure 6). The volume of sediment in the basin, bounded by granodiorite on the east, west, and south, and by the essentially impermeable till on the north, was then calculated by using the formula for the volume of the frustum of a cone:

$$V = 1/3 h (B_1 + B_2 + (B_1 B_2)^{1/2})$$

where B_1 and B_2 are the areas of the upper and lower bases of the frustum and h the vertical distance between them. Areas within each closed contour (the B's of the formula) were computed by superimposing the map on graph paper with cells 0.1 inch on a side (each cell representing an area of 2,500 square feet at the scale of the map) and counting the number of cells and fractions of cells within the contours. The results of the calculation are shown on Table I. The total volume calculated was 98.8×10^6 ft.³, or within the limits of error of the method, 100,000,000 ft.³ (2295.7 acre-feet). If the 50 percent of this volume that is sand and gravel has a specific yield of 15–20%, then the volume of available ground-water in the basin is 7,500,000 to 10,000,000 ft.³, or 172 to 230 acre-feet. This is the annual yield of the ground-water basin, on the assumption that the annual runoff from the drainage basin tributary to the ground-water basin would recharge the basin every spring. However, it would not be practicable to pump all the ground-water from the basin each year. This tributary drainage basin has an area of about 1,700 acres. According to the California Water Atlas (Kahrl et al., 1978) mean annual runoff from this part of the Sierra Nevada is 10 to 12 inches per year. Thus between 1400 and 1700 acre-feet of annual runoff is likely, 8 to 10 times the storage in the ground-water basin.

It must be cautioned that if a large fraction of the annual yield is drawn yearly out of the ground-water basin, lowering the water table well below the outlet to the meadow, this could cause Wolverton Creek to dry up for part of the year, as the meadow is recharged. It may also cause drastic changes in the vegetation of the meadow, e. g., replacement of meadow grasses and forbs by coniferous forest. The ground-water basin presently discharges into the creek, as shown by water-discharge measurements made by Jay Akers (oral communication, 1984).

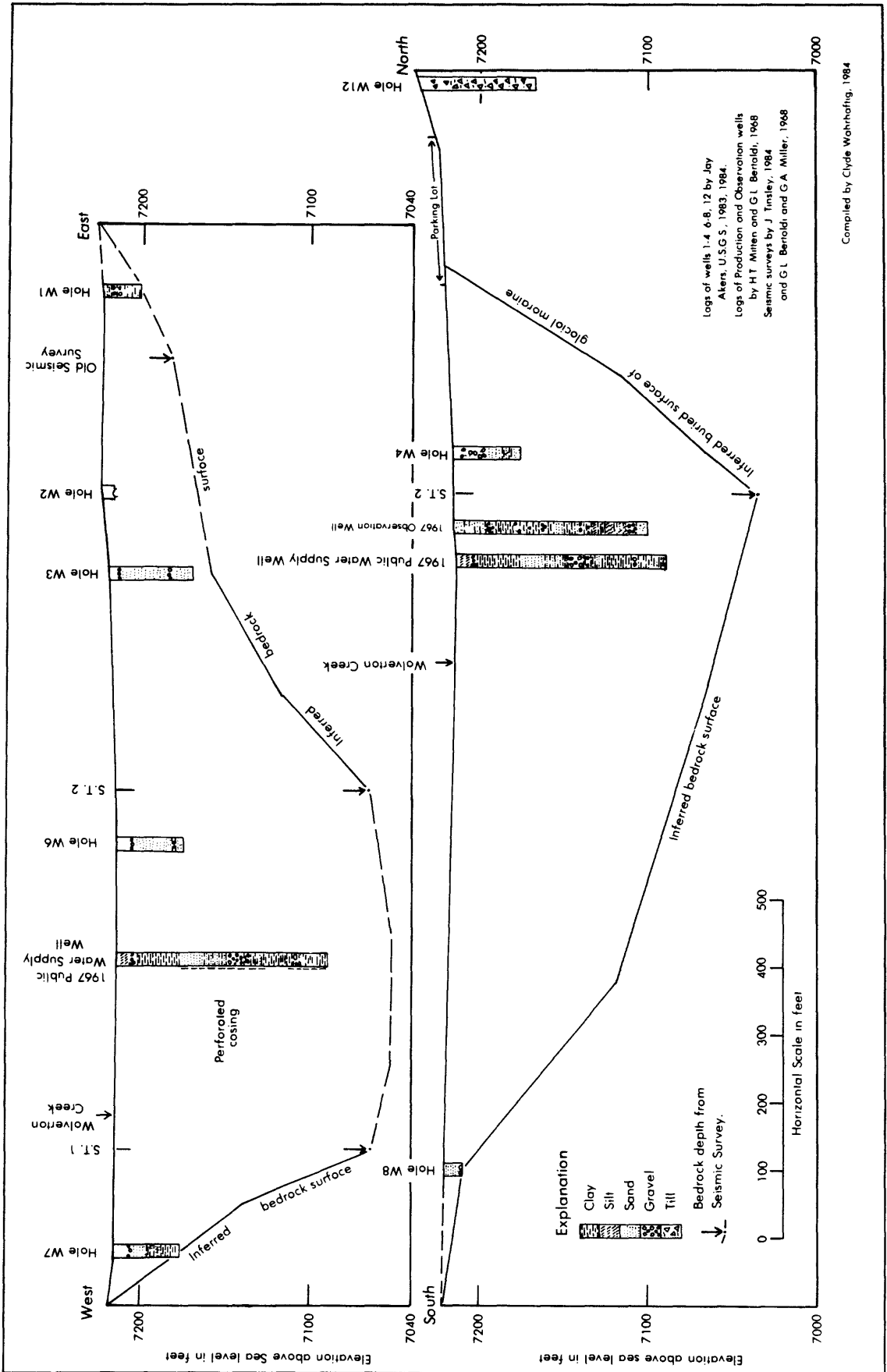


Figure 5 Vertical cross-sections of the alluvial basin at Wolverton, Sequoia National Park
Vertical scale 2.5 times Horizontal Scale. For location, see Figure 6.

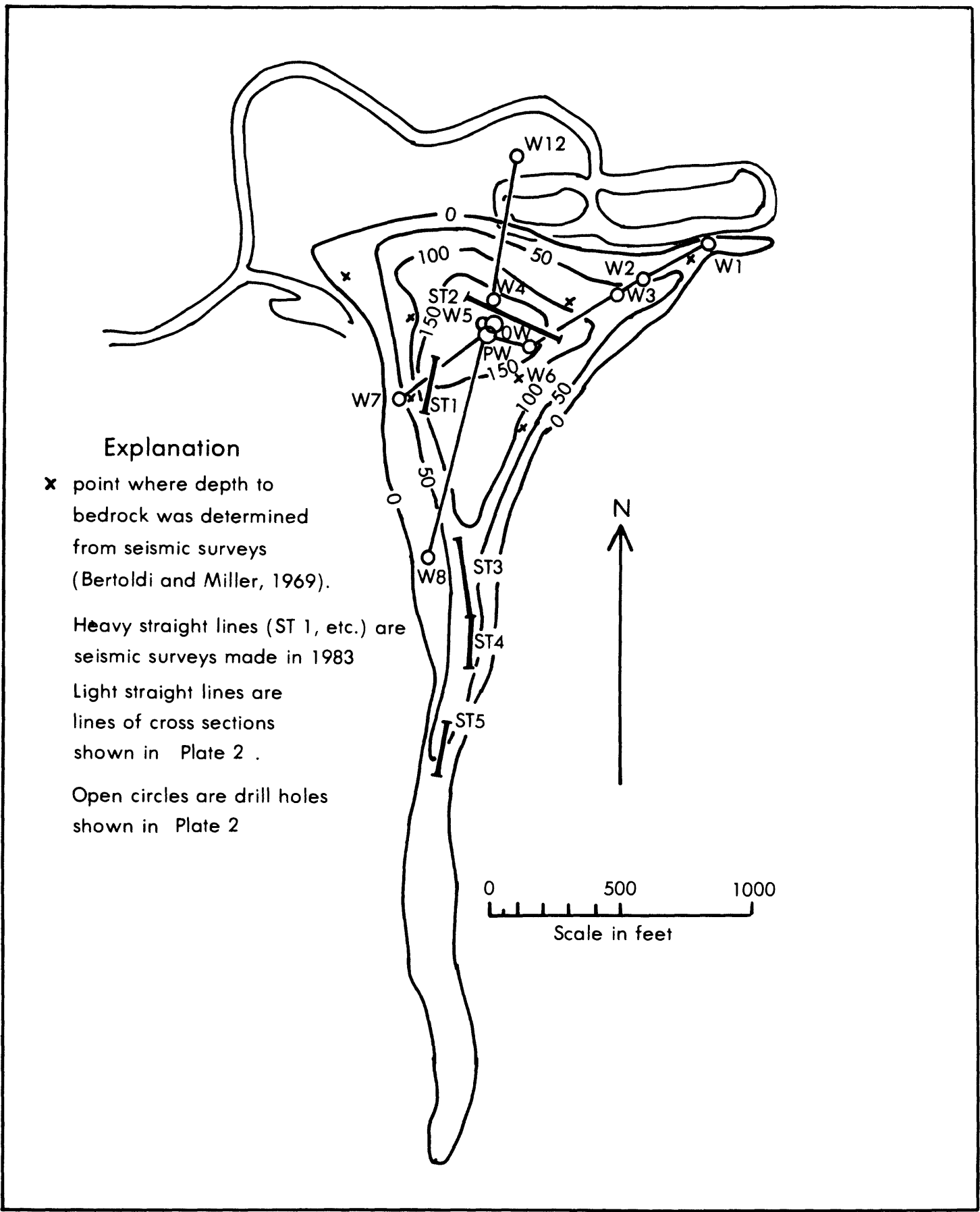


FIGURE 6. Contours on thickness of alluvial fill in basin at Wolverton, Sequoia National Park, California. Contour interval 50 feet. For location of wells, seismic survey lines, and roads, see Plate 2

TABLE I. CALCULATION OF VOLUME OF ALLUVIUM IN WOLVERTON GROUND-
WATER BASIN

Depth Contour (ft)	Area enclosed (ft ²)	$(B_1 B_2)^{1/2}$ (ft ²)	Volume between Contours (ft ³)
0	1.46×10^6	1.05×10^6	54.5×10^6
50	0.76×10^6	0.56×10^6	28.8×10^6
100	0.41×10^6	0.24×10^6	13.2×10^6
150	0.14×10^6	0	2.3×10^6
200	0		<hr/>
		Total	98.8×10^6

Note: Maximum depth is 200 feet.

Surficial geology and geomorphology of the Crescent Creek basin in relation to acid precipitation

The drainage basin of Crescent Creek above the outlet from Crescent Meadow and the drainage basin of Emerald Lake are two areas selected by the National Park Service for study of the impact of acid precipitation in Sequoia National Park. The Geological Survey was asked informally by Park Service scientists (David Parsons, David Graber) to report on the geology of these two areas as background for the acid rain study. The bedrock geology of the Crescent Creek basin is described by Sisson and Moore (1984). The surficial geology, to the extent that it is known, is described here. The geology of the Emerald Lake drainage basin is covered in the next section.

In the limited time available for the study of surficial geology, the only field work done in the Crescent Creek basin was a seismic survey of the depth of alluvium beneath Crescent Meadow, and a traverse along Crescent Creek and the Sugar Pine Trail between Crescent Meadow and Moro Rock to study the nature of the outlet of Crescent Creek from its basin. A photogeologic study made of the basin and its environs, including most of the Giant Forest plateau, is shown in Figure 7. The aerial photographs used were National Park Service SEKI series Nos. 3-107 through 3-109, 3-112, 3-113, and 4-170 through 4-175, taken August 30, 1973, scale 1:15,840. These were studied using an Old Delft stereoscope, at magnifications of 1.5 times and 4.5 times, and all rock outcrops, wet meadows, and indications of jointing recognizable in the aerial photographs were plotted on a 1:24,000-scale orthophotomap and ultimately transferred to the base map of Figure 7. Locations of some rock outcroppings, not visible in the aerial photographs, were taken from strike-and-dip measurements plotted on the field sheets of T. Sisson and J. Moore for this project.

The entire upper basin of Crescent Creek, outlined in the long-and-short-dashed line of Figure 7, lies in the region of stepped topography (type 2) and outside the limits of recognizable glaciation. Its southern and eastern watersheds mark the boundary with the region of high straight steep slopes (topographic type 1, Figure 1), this part of the latter region being the north canyon wall of the Middle Fork of the Kaweah River.

The entire basin is underlain by the granodiorite of Giant Forest (Ross, 1958; Sisson and Moore, 1984). This rock is medium- to light grey medium-grained granodiorite. No modern studies of its mineral composition using stained slabs have yet been made. The only information on the mineral composition available is from Ross (1958, p 7-9; 12-13). This information is presented in Table 2, derived from Ross. None of Ross' samples was from the Crescent Creek drainage, and the six samples listed are from the Lodgepole-Wolverton area immediately north of the Crescent Creek basin. The chemical formulas of the minerals as given by Deer and others (1966) are listed in Table 3. Ross' mineral compositions were measured on thin-sections about 2 x 4 cm in area, compared with an average mineral grain diameter of 1-3 mm. As Ross notes, and the percentages in samples 37A and 37B (thin-sections from the same hand specimen) demonstrate, there is a great deal of variability in the measured mineral composition, probably in large part due to statistical variations arising from the small number of mineral grains (probably no more than 200) in each thin section.

TABLE 2. MINERAL COMPOSITIONS OF THIN-SECTIONS FROM THE GIANT FOREST PLUTON
(From Ross, 1958, p. 7-9)

Sample No.	Location	Plagioclase		K-feldspar	Quartz	Biotite	Hornblende
		Feldspar	An-content				
31	Generals Hwy W. of Silliman Cr.	50	40	16	19	10	5
35	Generals Hwy nr. Wolverton Cr.	37	40-27	27	27	5	4
36	Generals Hwy S. of mo. of Silliman Cr	47	40	18	20	8	7
37A	Hillside S. of Lodgepole store	31	45	30	27	8	4
37B	Same specimen	37	45	19	32	7	5
38	Near Wolverton	50	38	10	24	9	7
41	NE of Circle Mdw & S. of Long Mdw	49	35	11	26	10	4
Average of Giant Forest pluton		48	--	11	24	11	6
Range of Giant Forest pluton		30-75	18-48	tr.-40	10-35	4-14	0-10

The important thing to be derived from this table is that the rock is about 45 percent plagioclase feldspar with an anorthite (lime-bearing molecule) content of 30—45 percent, 20—30 percent quartz, and 5—10 percent biotite. Ross also notes that all the plutonic rocks show some alteration of plagioclase feldspar to a fine mixture of epidote minerals and calcite, of both feldspars to sericite (extremely fine-grained muscovite), and of biotite and hornblende to chlorite. These alterations are attributed to the reaction of hot ground-water with the minerals. The hot ground-water may have been residual from the crystallization of the magma that formed the pluton.

The granodiorite has numerous mafic inclusions (clots measuring a few inches to a foot across, and one to several feet in length, of fine-grained aggregates rich in dark minerals). The mafic inclusions are pancake- to rod-shaped and probably were deformed into these shapes when the presence of interstitial silicate liquid between the crystallizing minerals rendered the rock still plastic. In any one place the long and intermediate dimensions of most of the inclusions tend to have the same inclination, and strike (or trend) in the same direction, which is also parallel to the inclination and strike of the preferred orientation of the hornblende and biotite grains. This planar parallelism of mafic inclusions and dark minerals is called a foliation, and has been mapped systematically on Plate I. As shown on Plate I, it dips steeply throughout the entire pluton, and strikes south to slightly east of south in most of the Giant Forest plateau area, but has a more easterly strike in a half-mile-wide belt extending across the plateau just north of Circle Meadow.

At some time in the history of the rock, but long before it was exposed at the surface, the granodiorite was fractured along steep to vertical joints. Some of the joints could be recognized in the aerial photographs, where they cut broad outcrops. These are shown in heavy solid lines on Figure 7, and trend slightly east of north throughout most of the Giant Forest plateau, and almost due north-south or slightly east of south along the south rim, near Moro Rock. Long-continuous master joints are inferred to be responsible for the alignments of some streams and passes, and are shown with a heavy dot-dash line on Figure 7.

When the rock we see now was close to the surface, the unloading joints described in the section on stepped topography developed. These joints give the majority of the rock outcrops their smooth appearance, and account for the gently rounded shape of many of the hills in the Giant Forest Plateau. The smoothly rounded to nearly flat bedrock outcrops developed along unloading joints are here referred to as "bald rock" exposures.

Expansion of the sheets of rock between the unloading joints has kept most of the steep to vertical joints tightly closed, so that in general they can be detected only by close inspection on the ground. The few steep joints that could be recognized in the airphotos are probably visible because the relation of the unloading joints to topography allowed them to open.

Measurements were made of the proportions of the Crescent Creek basin identified in the photointerpretation as granodiorite outcrops and as wet meadows. Of the $44.7 \times 10^6 \text{ ft}^2$ in the basin, $5.36 \times 10^6 \text{ ft}^2$ or 12 percent was mapped as continuous "bald rock" outcrop, $720,000 \text{ ft}^2$ or 1.6 percent was mapped as scattered outcrops; and $1.44 \times 10^6 \text{ ft}^2$ or 3.2 percent was mapped as wet meadow. The remainder of the watershed is covered by dense coniferous forest, growing in a soil that is underlain by granodiorite weathered to gruss.

The seismic surveys in Crescent Meadow (see section on seismic refraction studies) were undertaken to learn the thickness of the gruss. They showed that solid bedrock is no more than 25 feet deep beneath the meadow and is commonly at shallower depths. Judging from the explanation of the origin of the stepped topography given in the preceding pages, the thickness of gruss is limited, and weathering to gruss probably does not extend more than a few feet below the permanent ground-water table. It may perhaps extend deeper along some of the through-going joints.

The ground-water reservoir in the Crescent Creek drainage is limited to this gruss, and to openings along joints, particularly along the unloading joints, which are probably spaced a few feet apart and confined to the uppermost 30 to 40 feet of bedrock. The lack of springs on the steep escarpment south and east of Crescent Meadow implies that there is little if any ground-water movement through deep joints or other fractures, and that all water falling on the basin is either returned to the air via evapotranspiration or is surface-runoff out of Crescent Meadow.

Since the bulk of the weathering of the granodiorite to gruss is mechanical weathering caused by expansion of the biotite grains, most of the minerals in the gruss are the primary minerals of granodiorite. Stevens and Carron (1948) have determined an "abrasion pH" for many minerals, which is the pH of water in contact with a crushed powder of the mineral. The abrasion pH's they determined for the common minerals to be expected in the gruss of Giant Forest and its weathering products are given in Table 3. As can be seen from this table, with the exception of quartz, montmorillonite, and kaolinite, which are slightly acid to neutral, the abrasion pH of the minerals in the gruss is distinctly alkaline. Hence the gruss should be a good buffering agent against excess acidity of soil water, and one would expect the pH of water seeping from the soil into streams and meadows to be controlled partly by this buffering action and partly by the acidifying action of soil CO₂.

TABLE 3. CHEMICAL FORMULAS AND ABRASION pH OF MINERALS THAT MAY BE PRESENT IN WEATHERED GRANODIORITE

<u>Mineral</u>	<u>Formula</u>	<u>Abrasion pH</u>
Primary Igneous		
Plagioclase	Mixtures of albite	
feldspars	and anorthite	
Albite	$\text{NaAlSi}_3\text{O}_8$	9, 10
Oligoclase	$\text{Ab}_{6-8}\text{An}_{4-2}$	9
Labradorite	$\text{Ab}_{4-2}\text{An}_{6-8}$	8, 9
Anorthite	$\text{CaAl}_2\text{Si}_2\text{O}_8$	8
K-feldspar	KAlSi_3O_8	8
(Orthoclase)		
Quartz	SiO_2	6, 7
Biotite	$\text{K}_2(\text{Mg}, \text{Fe}^{2+})_{6-4}(\text{Fe}^{3+}, \text{Al}, \text{Ti})_{0-2}\text{Si}_{6-5}\text{Al}_{2-3}\text{O}_{20}(\text{OH}, \text{F})_4$	10
Amphibole	$(\text{Na}, \text{K})_{0-1}\text{Ca}_2(\text{Mg}, \text{Fe}, \text{Al})_5(\text{Si}_{6-7}\text{Al}_{2-1}\text{O}_{22})(\text{OH}, \text{F})_2$	10
(Hornblende)		
Augite	$(\text{Ca}, \text{Na}, \text{Mg}, \text{Fe}, \text{Al}, \text{Ti})_2(\text{Si}, \text{Al})_2\text{O}_6$	10
Hydrothermal		
Chlorite	$(\text{Mg}, \text{Al}, \text{Fe})_{12}((\text{Si}, \text{Al})_8\text{O}_2)(\text{OH})_{16}$	7, 8, 9
Calcite	CaCO_3	8
Dolomite	MgCO_3	9, 10
Epidote	$\text{CaFe}^3.\text{Al}_2\text{O}.\text{OH}(\text{Si}_2\text{O}_7)(\text{SiO}_4)$	8
Muscovite	$\text{K}_2\text{Al}_4(\text{Si}_6\text{Al}_2\text{O}_{20})(\text{OH}, \text{F})_4$	7, 8
Weathering		
Smectite	$(1/2\text{Ca}, \text{Na})_{0.7}(\text{Al}, \text{Mg}, \text{Fe})_4((\text{Si}, \text{Al})_8\text{O}_{20})(\text{OH})_4.n\text{H}_2\text{O}$	6, 7
Vermiculite	$(\text{Mg}, \text{Ca})_{0.7}(\text{Mg}, \text{Fe}^3, \text{Al})_6((\text{Al}, \text{Si})_8\text{O}_{20})(\text{OH})_4.8\text{H}_2\text{O}$	8, 9
Kaolinite	$\text{Al}_4(\text{Si}_4\text{O}_{10})(\text{OH})_8$	5, 6, 7

Geology of Emerald Lake basin in relation to Acid Precipitation

by James G. Moore and Clyde Wahrhaftig

The bedrock and surficial geology of the Emerald Lake basin are shown in Figures 8 and 9. The bedrock geology was mapped in the field by James Moore and Thomas Sisson, who also mapped the deposits of Pleistocene till. A photogeologic study of the remainder of the surficial geology was made by Clyde Wahrhaftig, examining, with an Old Delft stereoscope with 1.5x and 4.5x magnifications, U. S. Geological Survey airphotos of Project VJZ, nos. 4-90 and 4-91, scale 1:47,000, taken August 27, 1955.

All the bedrock units are granitic and, with the exception of the granite of Lodgepole, are all relatively dark granodiorites that appear similar in the field. The granodiorites of Emerald Lake and Castle Creek have been separated out from the granodiorite of Giant Forest as mapped by Ross (1958) on the basis of sharp intrusive contacts with the granodiorite of Giant Forest and with each other. These three units, however, are similar mineralogically; they contain 12-20 percent dark minerals, and are generally medium grained and equigranular. The granodiorite of Mitchell Peak is also somewhat dark-colored, but contains larger crystals (up to 2 cm in size) of plagioclase and K-feldspar. A coarse-grained border zone has been mapped.

The granite of Lodgepole, which crops out over much of the area, is distinctly lighter in color with only about 2-7 percent dark minerals. It is rather coarse grained with widely spaced joints, and consequently is least susceptible to quarrying by glacial action. Several of the higher peaks, such as Panther Peak, Mt. Silliman, Tharp Rock, and Alta Peak, are underlain by this resistant rock.

During the glaciations of the Pleistocene the basin of the creek draining Emerald Lake was occupied by a glacier tributary to the Marble Fork glacier. During the height of the glaciations, ice filled the basin to within a few hundred feet of the tops of the surrounding ridges, and a continuous ice-field about 1,200 feet wide at its narrowest point separated Alta Peak from the south end of the nunatak ridge between Pear and Emerald Lakes. The firn limit on the north side of the Alta Peak-Panther Peak ridge was about 9,800 feet in altitude. The upper surface of the ice over Emerald Lake was about 9,800 feet in altitude or just about at the firn limit, assuming nearly straight ice-surface contours across this canyon. On this assumption, its thickness was 800 feet over Emerald Lake and the slope of its upper surface between Emerald and Aster Lakes was between 400 feet in 1600 feet and 400 feet in 1800 feet (0.25-0.22). The width of the glacier here was about 2,500 feet. Applying the techniques of Nye, as described by Paterson (1969, p. 106, 107), a shear stress of 2.6-2.9 bars is calculated for the base of the ice at Emerald Lake, in contrast to a normally expected shear stress of 1-1.5 bars. This implies that the ice was thinner and that the glacier surface over the lake was concave (the thickness that would give about the correct basal shear stress at this surface slope would be about 400 feet).

The only till of Tioga (?) age mapped in the basin is a patch 600 feet long and 300 feet wide filling a trench along a master joint just northeast of Emerald Lake. From the photogeologic interpretation, the basin otherwise consists of bare granitic bedrock, with a few talus cones at the base of cliffs on the south and west sides. A patch of Holocene till was recognized in the photogeologic study. This patch is a fairly thin sheet of loose bouldery debris that masks the bedrock shelf at the base of the north wall of Alta Peak. This sheet is about 600 feet wide and 1800 feet long, and appears to bear low ridges parallel to its north edge. This sheet of till was probably left by a small cirque

glacier that probably existed at the base of Alta Peak during the Recess Peak glaciation 2,000—3,000 years ago. It appears to bury the south ends of lineations etched into the bedrock by ice of the Tioga glaciation along the traces of joints. Only the extreme west end of this till lies in the Emerald Lake basin.

The walls of the basin above the level of Tioga ice were subject to frost-riving and rockfall during Tioga time and subsequently. Post-glacial or Holocene frost-riving and rockfall produced the talus cones. The rock of the cliffs is therefore hard and fresh, probably as fresh as the bedrock floor of the basin.

The actual condition of the bedrock floor of the Emerald Lake basin is not known at first hand. If it is similar to the other glaciated cirques seen elsewhere in the Sierra Nevada, perhaps 5—20 percent of the floor is original glacially abraded surface, some of which may be glacial polish. Usually, however, such surfaces are underlain by a crack or very thin weathered zone parallel to the surface but separated by 5—10 mm of apparently fresh rock. Ultimately, the glacially abraded surface will spall off along this crack, leaving a roughened hackly bedrock surface, with numerous thin hairline cracks of limited extent, sub-parallel to the surface and intersecting it at very low angles. Water freezing in these fine cracks or hydrating the minerals along them pries off flakes of rock, keeping the surface fresh. The amount of lowering of the surface, based on the relief of preserved remnants of the glacially abraded surface, rarely exceeds one foot in the 10,000 years since ice left these cirques.

The unweathered rock presents a very limited surface area for contact with water, and reacts (or weathers) very slowly. Therefore, regardless of the abrasion pH of the minerals present, there is likely to be negligible buffering action of the rock, coarse angular talus, or till, in this basin, and the acidity of precipitation can be expected to be reflected quickly in the acidity of the lake and of other waters within this and similar bare rock basins.

The bare glaciated bedrock is impervious. Hence the only ground-water in the basin is in the patch of Tioga till, in the talus cones, and beneath meadows around the lake or in tiny alluvium-filled basins carved in bedrock. Water storage in this basin is therefore essentially in snowbanks that persist into the summer or early fall and in the lakes.

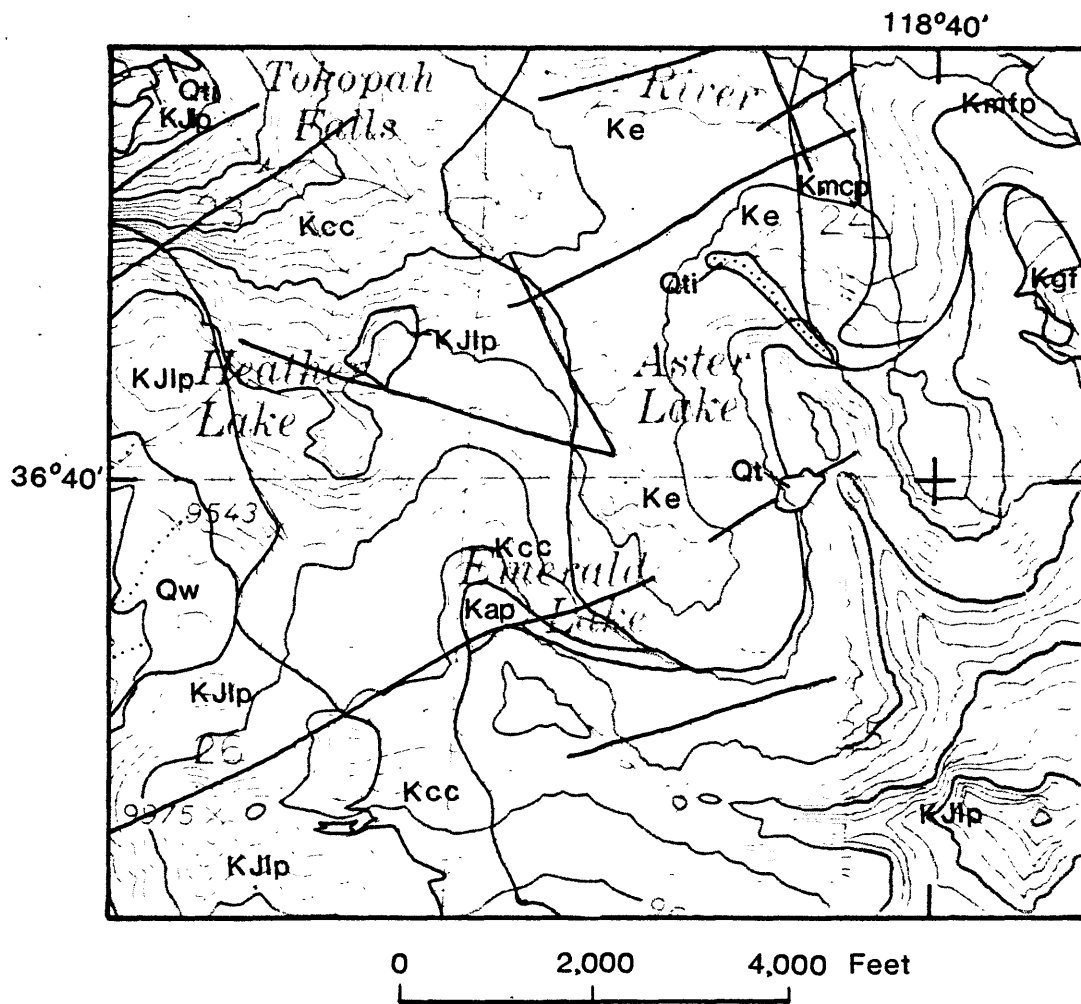


**Figure 8.- Bedrock Geology of the Emerald Lake cirque
and vicinity
Sequoia National Park**

by James G. Moore

For explanation of symbols, see Plate L. Diagonal lines are prominent linear features recognized in aerial photographs, and are probably traces of major joints.

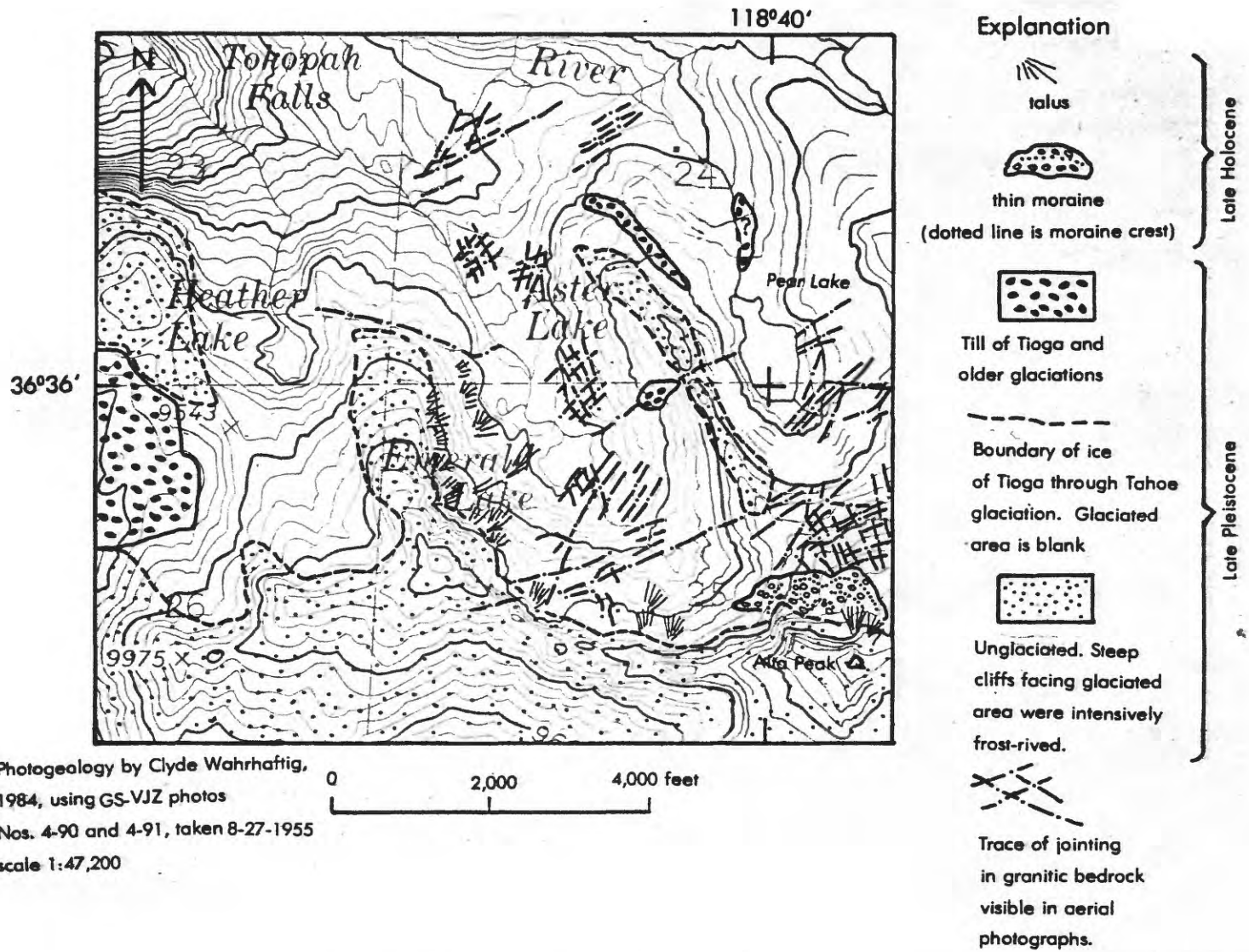


Figure 9. Surficial photogeologic reconnaissance map of Emerald Lake and vicinity, Sequoia National Park, Calif.

Seismic Refraction Studies of the
Thickness of Valley Fill in
Wolverton Ground Water Basin and beneath Crescent Meadow,
Sequoia and Kings Canyon National Parks, California

by

John C. Tinsley

Introduction

We conducted seismic refraction surveys at selected points in the Wolverton ground water basin and at Crescent Meadow during September 14-17, 1983, in order (1) to obtain improved estimates of the volume of ground water stored in the valleys by determining the thickness of water-saturated alluvial fill and (2) to obtain information on the nature of the underlying bedrock based on measured velocities of compressional (P-wave) seismic waves.

Seismic waves are essentially sound waves travelling through the earth. The greater the density and firmness of a substance, the faster seismic (i.e., sound) waves travel through it. The effects of these properties of the substances under consideration can be appreciated by keeping in mind that the velocity of sound in air is about 1100 feet per second.

Equipment

The seismic surveys were conducted using Bison Model 1580 and 1575-B Signal-Enhancement Seismographs. These portable systems consist of a hammer and an array of detectors linked by wires to a self-contained timer equipped with a cathode-ray tube (CRT) and viewing screen on which the seismic signals are displayed. The seismic signal is generated at a given distance from the detector by a series of blows struck with a 16 lb sledge hammer. The impact of the hammer on an aluminum plate closes an inertial relay on the hammer which starts the timer. The P-waves generated are recorded by geophone detectors and are electrically added by the machine. The resulting waveform is displayed on the CRT. The velocity of the impulse through the earth materials is computed from measurements of travel-times and respective distances that separate the hammer-point and the detectors.

Technique

Standard hammer-powered seismic refraction techniques were used. The hammer point can be shifted relative to the geophone detectors or vice-versa. In this survey, waterproof or submersible geophones were pressed firmly about 10 cm into the meadow's vegetal mat forming a linear array of stations at measured intervals from the hammer-station. At the hammer-station, an aluminum plate was placed on the ground surface, the plate was struck one or more times with the hammer, and the travel-time of the P-wave phase was determined from the waveforms recorded and displayed on the CRT. The travel times and corresponding distances for each survey are presented in Tables 4.

The principles behind the interpretation of the seismic results are briefly summarized from Dobrin, 1976, p.34-43; 294-298 (see Figure 10). Figure 10-a is a cross-section of very simple conditions beneath the ground, where a uniformly thick layer of a

substance through which seismic (sound) waves travel with a velocity V_1 overlies a substance through which seismic waves travel with velocity V_2 . The interface between these two substances is planar and parallel to the ground surface. The hammer station is at point A, and detectors are located at points D_1, D_2, D_3 , etc. When the hammer strikes the plate, a sharp seismic wave-front radiates into the ground at velocity V_1 , occupying successively the hemispherical shells whose cross-sections are the half-circles shown by light lines in the diagram. When the seismic wave reaches the interface, the wave energy travels through the lower substance at the faster velocity V_2 . The directions of the perpendiculars (called rays) to the wave-fronts—perpendiculars that are the paths of the seismic waves—change at the interface in keeping with Snell's Law, illustrated in Figure 10-b, which is as follows:

$$\frac{\sin i}{\sin r} = \frac{V_1}{V_2}$$

where i is the angle of the incident ray and r is the angle of the refracted ray, both angles measured against the perpendicular to the interface. (Snell's Law is the law which accounts for the fact that a straight inclined stick plunged partly into water appears to bend at the water surface, and for the ability of lenses to magnify, of eyeglasses to improve our eyesight, and of our eyes to see. Light and sound are both wave phenomena, and Snell's Law applies to all wave phenomena.)

When $\sin r$ equals 1 (i. e., when $\sin i = V_1/V_2$), the wave-front in the lower substance is perpendicular to the interface and the seismic wave travels along the interface with the velocity V_2 . The angle of incidence for which this is true is called the critical angle, i_c . As the wave front moves along the interface, it generates seismic energy in the upper substance, which travels back toward the surface with the velocity V_1 . It can be shown mathematically that the first of this secondary seismic energy to reach the ground surface at any point has a return path that makes the critical angle of incidence, i_c , with the perpendicular to the interface.

As the first sound wave in the upper substance reaches the detectors at D_1, D_2, \dots, D_6 , they record its arrival times T_1, T_2, \dots, T_6 . The sound waves that travel down to the second medium at B, and return to the surface from C_7, C_8 , and C_9 , reach the detectors D_7, D_8 , and D_9 , before the sound waves along the surface, because the faster velocity in the lower medium more than makes up for the greater distance the former must travel. The differences in the arrival times between these more distant detectors are governed by the faster velocity through the lower substance, because the distances $C_7-D_7, C_8-D_8, C_9-D_9$ are all equal, and also equal to A-B.

The arrival times at detectors D_1, D_2, \dots, D_6 are simply $T_u = x/V_1$, where x is the distance to the detector from the hammer station. The arrival times at detectors D_7, D_8 , and D_9 , however, are the sums of three times:— (1) the time taken to go from A to B; (2) the time from B to C_7, C_8 , or C_9 , and (3) the time to travel C-D, which is the same as the time to travel A-B. This total travel time is

$$T_b = \frac{2z}{V_1 \cos. i_c} + \frac{x - 2z \tan. i_c}{V_2}$$

where z is the depth to the interface.

The arrival times and distances are plotted on a time-distance graph, shown on Figure 10-c, where time is plotted on the vertical axis and distance is plotted on the horizontal axis. The graph consists of two straight-line segments. The inverse slope of

the near segment, $(x_2 - x_1)/(T_2 - T_1)$, is the velocity V_1 in the upper substance. The inverse slope of the far segment, $(x_9 - x_8)/(T_9 - T_8)$, is the higher velocity in the lower substance. The value of \underline{x} at the intersection of these two straight-line segments is the crossover distance, x_{cr} . If the farther straight-line segment of the travel-time graph is extended back to the T axis (where $\underline{x} = 0$) the value of T so determined is T_i , the intercept time.

If, using the trigometric identities, one substitutes the values in terms of V_1 and V_2 for the cosine of i_c , $(1 - V_1^2/V_2^2)^{1/2}$, and its tangent, $V_1/(V_2^2 - V_1^2)^{1/2}$, into the equation for T_b , the value of T_b for $\underline{x} = 0$ (i. e., the intercept time) is found to be

$$T_i = 2z \frac{(V_2^2 - V_1^2)^{1/2}}{V_1 V_2}$$

and

$$z = \frac{T_i V_1 V_2}{2 (V_2^2 - V_1^2)^{1/2}}$$

or, since $T_u = T_b$ at the crossover distance, the values for the two times can be equated, and the depth found to be equal to $1/2 x_{cr} ((V_2 - V_1)/(V_2 + V_1))^{1/2}$.

The mathematics of the theory are much more complicated for the situation where the interface is not parallel to the ground-surface, but the principles involved are the same. The actual conditions at Wolverton and Crescent Meadow probably depart considerably from the ideal model used to demonstrate the principles involved. The interface between the alluvium and bedrock is not level nor plane, but, as Figure 6 shows, quite irregular. The contact may not be sharp, for the uppermost bedrock is probably weathered, and has seismic velocities between that of alluvium and fresh bedrock. The overlying alluvium probably does not have a uniform seismic velocity, but consists of layers and lenses of gravel, sand, and clay, which all have different seismic velocities. The problems that can result from these variations in the character of the rock materials and their interfaces are described by Domzalski (1956). In particular, if a hidden low-velocity layer underlies a higher-velocity surface layer, the analysis of the data would give an erroneously great depth to bedrock, and there would be no way of recognizing this fact, solely from seismic refraction studies. A boring or well drilled through the alluvium to bedrock would be required to obtain definitive data in this instance.

Reversed Versus Non- Reversed Profiles

A refraction profile based on a record made with the hammer at one end only of the linear geophone array is called an unreversed profile. If two records are made of a single linear geophone array, with the hammer point at a different end for each record, the resulting profile is termed a reversed profile. Unreversed hammer-powered P-wave refraction profiles are sufficient to determine the thickness of the alluvial fill and the depth to any abrupt changes in seismic velocity within it, as well as the seismic velocities in the fill and underlying bedrock, down to a depth of about 300 ft. This was the information sought. If one wishes to know the slope of the basin floor beneath the alluvium, and the direction in which the basin floor is sloping, two reversed profiles running perpendicular to each other are needed at each point where this information is

sought. Time was not available to do this routinely, and only one profile at each of the two study areas was reversed. In general, the alluvial thicknesses calculated for each profile are valid along an interval centered near the midpoint of the profile.

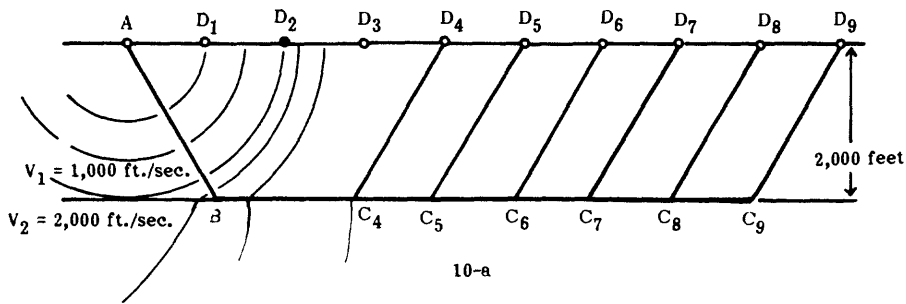
Results - Wolverton Ground Water Basin

Five refraction profiles were recorded in Wolverton Meadow and the data and the results are shown in Table 4. These profiles were located as shown in plate 2 and figure 6. The apparent thicknesses of valley fill are shown in the cross sections (figure 5). These profiles indicate that the apparent P-wave velocities which characterize both the valley fill and the subjacent granitic plutonic rock range from 1200 to 2600 ft/sec for unsaturated and partly saturated alluvium; from 4900 to 5300 ft/sec for water-saturated alluvium; and from 15000 to 40000 ft/sec for the crystalline plutonic (granitic or granodioritic) bedrock. Computed maximum apparent thicknesses of water-saturated alluvial fill are about 200 ft (see figure 6) The alluvium thins gradually to the east and to the south where thickness of 50-60 ft occur near the axis of Long Meadow.

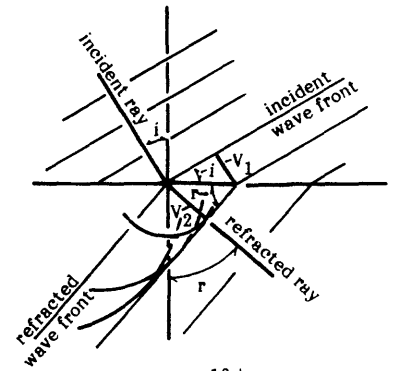
Results - Crescent Meadow

Four refraction surveys were conducted in Crescent Meadow and the data and the results are shown in table 4. The locations of these surveys are shown in figure 7. Geologic studies plus these geophysical studies indicate that the alluvial fill is relatively thin beneath Crescent Meadow. Alluvial thicknesses in Crescent Meadow range from 5 ft to as much as 25 ft and change rapidly depending upon the configuration of the granitic rock beneath the meadow. Apparent seismic velocities range from 1060(?) to 2500 ft/sec for unsaturated or partly saturated alluvium; from 4900-5600 for water-saturated alluvium.

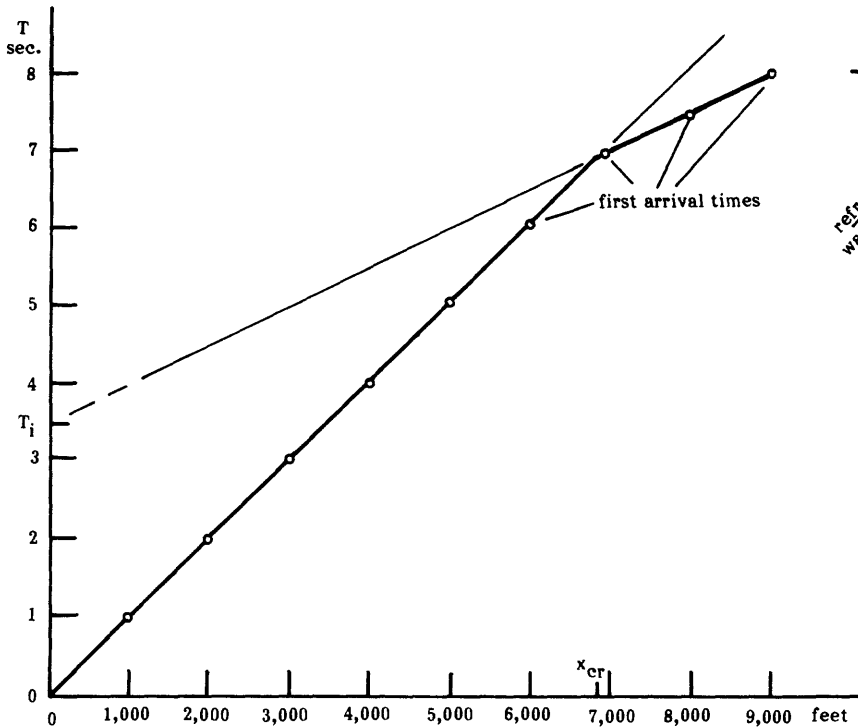
Profiles 2a and 2b suggest that an appreciable thickness (about 35 ft) of compact but weathered or fractured mantle above hard relatively unweathered granite is present locally in Crescent Meadow that was not detected in the other Crescent Meadow seismic profiles. However, the water-bearing characteristics of this horizon were not evaluated. A bedrock riser exposed in the streambed issuing from Crescent Meadow also suggests the valley fill is not very thick. The elevation of the bedrock lip relative to the surface of Crescent Meadow, plus the geophysical studies indicate that Crescent Meadow contains only a thin valley fill, probably less than 10 ft thick in most areas.



10-a



10-b



10-c

Figure 10. Diagrams illustrating the principles of refraction seismic measurements of depth to bedrock. 10-a, cross-section of a 2,000-ft.-thick layer of alluvium with seismic velocity of 1,000 ft. per second overlying bedrock with seismic velocity of 2,000 ft. per second, on a horizontal interface parallel to the ground surface, showing wave-fronts and ray paths; 10-b, Huygens diagram illustrating Snell's Law, shown for a plane wave-front. Fine lines sloping to the left represent positions of a single wave at successive equal intervals of time, where $V_2 = 1.5V_1$; the refracted wave front is the common tangent to hemispheres along the interface whose wave energy travels into the lower substance at the velocity V_2 , generated by the wave-front as it passes along the interface; 10-c, travel-time curve constructed for seismic survey conducted in the geologic setting shown in 10-a.

Table 4. Results of Seismic Refraction Surveys

WOLVERTON No. 1 (Locality ST-1, Plate 2)										Azimuth 191°		
Distance (ft)	30	60	90	120	150	180	210	240	270	300		
Time of First Arrival (sec x 10 ⁻³)	18.8	26.0	29	36.4	43.6	48.5	55.6	61.2	65.6	69.0		
LAYER NUMBER	APPARENT VELOCITY (ft/sec)		APPARENT THICKNESS (ft)		PROBABLE MATERIAL							
1	1600		5		Alluvium, partly saturated							
2	5200		74		Alluvium, water-saturated							
3	7700		71		Older alluvium (?), water-saturated, or granitic rock, weathered							
4	15000 (assumed)				Granitic rock, unweathered							
Thickness of younger water-bearing valley fill						79 ft						
Thickness of weathered mantle						71 ft						
Minimum depth to unweathered(?) granitic rock						150 ft		Accuracy = ± 5%.				
WOLVERTON No. 2 (Locality ST-2, Plate 2)										Azimuth 270°		
East to West												
Distance (ft)	30	60	90	120	150	180	210	240	270	300	330	360
Time of First Arrival (sec x 10 ⁻³)	23.2	28.0	32.8	38.0	44.6	49.2	53.3	61.2	68.5	70.5	75.2	76.0
West to East												
Time of First Arrival (sec x 10 ⁻³)	18.5	26.4	30.8	38.0	43.2	48.0	53.2	61.6	66.4	69.6	71.2	74.5
LAYER NUMBER	APPARENT VELOCITY (ft/sec)		APPARENT THICKNESS (ft)		PROBABLE MATERIAL							
			(East)	(West)								
1	1500		14	11	Alluvium, partly saturated							
2	5200		135	190	Alluvium, saturated							
3	15000		---	---	Granitic rock							
Depth to granitic rock		150	200	Accuracy = ± 5%.								
WOLVERTON No. 3 (Locality ST-3, Plate 2)										Azimuth 350°		
Distance (ft)	25	50	75	100	125	150	175	200	225	250	275	300
Time of First Arrival (sec x 10 ⁻³)	9.5	17.0	22.2	24.0	29.0	34.5	39.5	42.9	50.0	51.5	51.7	52.0
LAYER NUMBER	APPARENT VELOCITY (ft/sec)		APPARENT THICKNESS (ft)		PROBABLE MATERIAL							
1	2600		8		Alluvium, partly saturated							
2	4900		97 (82)		Alluvium, saturated							
3	40,000 (20,000)		-----		Granitic rock							
Depth to granitic rock = 90-105 ft, depending on the velocity attributed to bedrock												
Accuracy = ± 5%												

Table 4 continued.

WOLVERTON No. 4 (Locality ST-4, Plate 2) Azimuth 180°

Distance (ft)	25	50	75	100	125	150	175	200
Time of First Arrival (sec x 10 ⁻³)	9.8	14.3	19.4	24.0	28.8	32.3	34.0	35.7

LAYER NUMBER	APPARENT VELOCITY (ft/sec)	APPARENT THICKNESS (ft)	PROBABLE MATERIAL
1	2550	7	Alluvium, partly-saturated
2	5200	47	Alluvium, saturated
3	14,700		Granitic rock

Depth to granitic rock = 54 ft
Accuracy = ± 5%

WOLVERTON No.5 (locality ST-5, Plate 2) Azimuth 195°

Distance (ft)	25	50	50	100	125	150	175	200	225
Time of First Arrival (sec x 10 ⁻³)	8.5	13.4	19.9	23.4	27.6	32.5	34.0	35.8	36.5

LAYER NUMBER	APPARENT VELOCITY (ft/sec)	APPARENT THICKNESS (ft)	PROBABLE MATERIAL
1	1200	3	Alluvium, partly-saturated
2	5270	53	Alluvium, saturated
3	18,100	-----	Granitic rock

Depth to granitic rock = 56 ft
Accuracy = ± 5%

CRESCENT MEADOW No 1a (Locality C-1, figure 7) Azimuth = 162°

Distance (ft)	10	20	30	35	40	50	60	70	80
Time of First Arrival (sec x 10 ⁻³)	7.8	17.4	26.7	29.0	11.5	13.9	14.7	16.3	17.1

LAYER NUMBER	APPARENT VELOCITY (ft/sec)	APPARENT THICKNESS (ft)	PROBABLE MATERIAL
1	1060	5-13	Alluvium, water-saturated
2	8300	-----	Granitic Rock, weathered and/or fractured

Thickness of water-bearing valley fill is less than 13 ft.
Accuracy = ±5%.

Table 4 continued.

CRESCENT MEADOW No. 1b (Locality C-1, figure 7) Azimuth 158°

Distance (ft)	5	10	25	50	75	100	125	150
Time of First Arrival (sec x 10 ⁻³)	4.5*	6.0	8.6	13.2	17.4	18.4	21.0	22.4

LAYER NUMBER	APPARENT VELOCITY (ft/sec)	APPARENT THICKNESS (ft)	PROBABLE MATERIAL
1	1100	2	Alluvium, water-saturated; *airborne accoustical impulse obscured first arrival of P-wave.
2	5600	23	Alluvium, water-saturated.
3	12,500	-----	Alluvium, water-saturated Granitic rock, unweathered

Thickness of water-bearing valley fill = 25 ft.
Accuracy = ±5%

CRESCENT MEADOW No. 2 (Locality C-2, figure 7) Azimuth 90°

West to East

Distance (ft)	5	10	25	50	75	100	125	150
Time of First Arrival (sec x 10 ⁻³)	4.0	4.6	6.5	9.0	11.7	14.0	17.0	19.3
East to West	3.0	4.0	7.1	11.1	14.4	17.1	18.5	19.5

LAYER NUMBER	APPARENT VELOCITY (ft/sec)	APPARENT LAYER THICKNESS (ft)	PROBABLE MATERIAL
1	2500	5	Alluvium, water saturated
2	8600	35	Granitic rock, weathered
3	20,800	-----	Granitic rock, unweathered.

Depth to weathered granitic rock = 5 ft.
Depth to unweathered granitic rock = 40 ft.
Accuracy = ±5%.

CRESCENT MEADOW No. 3 Locality C-2, figure 7) Azimuth 162°

Distance (ft)	5	10	20	30	40	50
Time of First Arrival (sec x 10 ⁻³)	3.6	4.7	6.8	8.8	10.0	11.0

LAYER NUMBER	APPARENT VELOCITY (ft/sec)	APPARENT THICKNESS (ft)	PROBABLE MATERIAL
1	1400	2	Peat & vegetal matter
2	4900	9	Alluvium, water-saturated
3	10,000	-----	Granitic rock, weathered or fractured

Thickness of water-bearing valley fill = 11 ft.
Minimum Depth to unweathered granitic rock = 11 ft.
Accuracy = ±5%

References Cited

- Adam, David P., in press, Quaternary Pollen Records from California, in Lippold, Lois K., ed., Proceedings of the Symposium on "Holocene Climate of the California Coast and Desert", San Diego State University, February 12-13, 1982.
- Akers, Jay P., 1984, The Relation of Ground Water in the Wolverton Valley area with that in the General Sherman Tree area, Sequoia National Park, California; U. S. Geological Survey Water Resources investigations Report No. 84-XXX, XXX pages.
- Bailey, Roy A., G. Brent Dalrymple, and Marvin A. Lanphere, 1976, Volcanism, structure, and geochronology of Long Valley Caldera, Mono County, California; Journal of Geophysical Research, vol. 81, No. 5, Feb. 10, 1976, p. 725-744.
- Batchelder, George L., 1980, A late Wisconsinan and early Holocene lacustrine stratigraphy and pollen record from the west slope of the Sierra Nevada, California (abstr.); Program and Abstracts, American Association for Quaternary Research (AMQUA), 6th Biennial meeting, 18-20 Aug., 1980.
- Bateman, Paul C., and Wahrhaftig, Clyde, 1966, Geology of the Sierra Nevada, in Geology of Northern California, Edgar H. Bailey, ed., California Division of Mines and Geology Bull. 190, p. 107-172.
- Berggren, W. A., L. H. Burckle, M. B. Ciuta, H. B. S. Cooke, B. M. Funnell, S. Gartner, J. D. Hays, J. P. Kennett, N. D. Opdyke, L. Pastouret, N. J. Shackleton, and Y. Takayanagi, 1980, Toward a Quaternary Time Scale; Quaternary Research, vol. 13, p. 277-302.
- Bertoldi, Gilbert L., and Miller, G. A., 1969, Geophysical Survey and Pumping Test in Wolverton Creek Valley, Giant Forest Area, Sequoia National Park, California; U. S. Geological Survey, Water-Resources Division, Administrative Report No. 6420-05, 17 pages.
- Birkeland, Peter W., 1964, Pleistocene glaciation of the Northern Sierra Nevada, north of Lake Tahoe, California; Journal of Geology, vol. 72, No. 6, p. 810-825.
- Birkeland, Peter W., Dwight R. Crandell, and Gerald M. Richmond, 1971, Status of correlation of Quaternary Stratigraphic Units in the western Conterminous United States; Quaternary Research, vol. 1, No. 2, p. 208-227, two tip-in charts.
- Birman, J. H., 1962, Glaciation of Parts of Sequoia and Kings Canyon National Parks, Sierra Nevada, California; Administrative report in the files of the National Park Service, Sequoia National Park, 27 pages, 15 figures.
- Birman, Joseph H. 1964, Glacial Geology across the crest of the Sierra Nevada, California; Geological Society of America Special Paper 75, 80 pages, 1 plate in pocket
- Blackwelder, Eliot, 1931 Pleistocene glaciation in the Sierra Nevada and the Basin Ranges; Geological Society of America Bull., Vol. 42, No. 4, p. 865-922.
- Colman, Steven M., and Pierce, Kenneth L., 1981, Weathering Rinds in Andesite and Basalt Stones as a Quaternary Age Indicator, Western United States; U. S. Geological Survey Professional paper 1210, 56 pages.

- Cox, Allan, ed., 1973, *Plate Tectonics and Geomagnetic Reversals*; San Francisco, W. H. Freeman and Company, 702 pages.
- Croft, M. G., 1966, revised 1968, *Ground-water reconnaissance of the Giant Forest area, Sequoia National Park, California*; U. S. Geological Survey, Water-Resources Division, Administrative Report to the National Park Service, 5 pages; with an 8-page appendix by H. T. Mitten and G. L. Bertoldi.
- Curry, Robert R., 1966, *Glaciation about 3,000,000 years ago in the Sierra Nevada*; *Science*, vol. 154, no. 3750, p. 770—771.
- Curry, Robert R., 1971, *Glacial and Pleistocene history of the Mammoth Lakes Sierra—a geologic guidebook prepared in conjunction with the Sept. 11-12, 1971, field conference of the Pacific Coast Section, Friends of the Pleistocene*; Missoula, Montana, University of Montana Department of Geology, 49 p., 1 map.
- Deer, W. A., R. A. Howie, and J. Zussman, 1966, *An Introduction to the Rock-forming Minerals*; London, Longmans Group Limited, 528 pages.
- Dobrin, M. B., 1976, *Introduction to geophysical prospecting*, 3rd edition, New York: McGraw-Hill Book Company, 632 p.
- Domzalski, W., 1956, *Some problems of shallow refraction investigation: Geophysical Prospecting*, v. 4, p. 140-166.
- Gilbert, G. K., 1904, *Domes and dome structure of the High Sierra*; *Geological Society of America Bulletin*, vol. 15, p. 29-36, plates 1-4.
- Gillespie, Alan Reed, 1982, *Quaternary Glaciation and Tectonism in the southeastern Sierra Nevada*; Thesis submitted in partial fulfillment of the requirements for the degree of Doctor of Philosophy, California Institute of Technology, Pasadena, Calif., 695 pages, 2 plates in pocket. (Available from Alan Gillespie, Jet Propulsion Laboratory, Pasadena California).
- Glen, William, 1982, *The Road to Jaramillo—Critical Years of the Revolution in Earth Science*; Stanford, Stanford University Press, xvii + 459 pages.
- Harden, Jennifer W., 1982, *A quantitative index of soil development from field descriptions: Examples from a chronosequence in central California*; *Geoderma*, vol. 28, p. 1—28.
- Harland, W. B., A. V. Cox, P. G. Llewellyn, C. A. G. Pickton, A. G. Smith, and R. Walters, 1982, *A Geologic Time Scale*; Cambridge University Press, 131 p., chart.
- Harwood, David S., Helley, Edward J., and Doukas, Michael P., 1981, *Geologic Map of the Chico Monocline and northeastern part of the Sacramento Valley, California*; U. S. Geological Survey Misc. Geologic Investigation Map I-1238, 1:62,500.
- Hay, Richard L., 1964, *Phillipsite of Saline Lakes and Soils*; *American Mineralogist*, vol. 49, No. 9-10, p. 1366-1386

- Huber, N. King, 1981, Amount and timing of late Cenozoic uplift and tilt of the central Sierra Nevada, California—Evidence from the upper San Joaquin River basin; U. S. Geological Survey Professional Paper 1197, 28 pages.
- Jahns, Richard H., 1943, Sheet structure in granite, its origin and use as a measure of glacial erosion in New England; *Journal of Geology*, Vol. 51, p. 71—98.
- Kahrl, William L., editor, 1978 (1979), *The California Water Atlas*; prepared by the Governor's Office of Planning and Research in cooperation with the California Department of Water Resources, 118 pages, folio. Available from General Services, Publication Section, P. O. Box 1015, North Highlands, California, 95660, or William Kaufmann, Inc., Los Altos, California.
- Liddicoat, Joseph C., Neil D. Opdyke, and George I. Smith, 1980, Paleomagnetic Polarity in a 930-m core from Searles Valley, California; *Nature*, vol. 286, No. 5768, p. 22-25, July 3, 1980.
- Lindgren, Waldemar, 1911, *The Tertiary Gravels of the Sierra Nevada of California*; U. S. Geological Survey Professional Paper 73, 226 pages.
- Lockwood, J. P., and Moore, James G., 1979, Regional deformation of the Sierra Nevada, California, on conjugate microfault sets; *Journal of Geophysical Research*, vol. 84, p. 6041—6049.
- Mankinen, E. A., and Dalrymple, G. B., 1979, Revised geomagnetic polarity time scale for the interval 0-5 m. y. B. P.; *Journal of Geophysical Research*, vol. 84, No. B2, p. 615-626.
- Marchand, Denis E., 1977, The Cenozoic History of the San Joaquin Valley and adjacent Sierra Nevada, as inferred from the geology and soils of the Eastern San Joaquin Valley; p. 39-50 and fig. 9 in *Soil Development, Geomorphology, and Cenozoic History of the Northeastern San Joaquin Valley and Adjacent Areas, California: A guidebook for the joint field session of the American Society of Agronomy, Soil Science Society of America, and the Geological Society of America, Nov. 10-11, 1977* by Gordon L. Huntington, Eugene L. Begg, Jennifer W. Harden, and Denis E. Marchand, edited by Michael J. Singer, 328 pages.
- Marchand, Denis E., and Allwardt, Alan, 1981, Late Cenozoic Stratigraphic Units, Northeastern San Joaquin Valley, California; U. S. Geological Survey Bulletin 1470, 70 pages, 2 plates in pocket.
- Matthes, Francois E., 1930, *Geologic History of the Yosemite Valley, with an appendix on the granitic rocks of the Yosemite region* by F. C. Calkins; U. S. Geological Survey Professional Paper 160, 137 pages, 52 plates (3 in pocket).
- Matthes, Francois E., 1965, *Glacial reconnaissance of Sequoia National Park, California*; prepared posthumously by Fritiof Fryxell from Matthes' notes and other sources; U. S. Geological Survey Professional Paper 504-A, ix + p. A1—A58; plates 1 and 2 in pocket
- Meyer, C. E., M. J. Woodward, A. M. Sarna-Wojcicki, and C. W. Naeser, 1980, Zircon fission-track age of 0.45 million years on ash in the type section of the Merced Formation, west-central California; U. S. Geological Survey Open-File Report No. 80-1071, 9 p.

- Oberlander, T. M., 1972, Morphogenesis of Granitic Boulder Slopes in the Mojave Desert, California; *Journal of Geology*, Vol. 80, No. 1, p. 1—20.
- Packer, Duane R., Jefferson R. McCleary, Victor O. Cherven, and Raymond L. Blum, 1977, Paleomagnetic Investigations of the Turlock Lake Formation at the Type Section, p. 267-275 in *Soil Development, Geomorphology, and Cenozoic History of the Northeastern San Joaquin Valley and adjacent areas, California: A Guidebook for the Joint Field Session of the American Society of Agronomy, Soil Science Society of America, and Geological Society of America*, Nov. 10-13, 1977, by Gordon L. Huntington, Eugene L. Begg, Jennifer W. Hardin, and Dennis E. Marchand, edited by Michael J. Singer, 328 pages.
- Paterson, W. S. B., 1969, *The Physics of Glaciers*; Oxford, Pergamon Press, 250 pages.
- Ross, Donald E., 1958, *Igneous and Metamorphic Rocks of parts of Sequoia and Kings Canyon National Parks, California*; Calif. Division of Mines, Special Report 53, 24 pages, 1 plate in pocket.
- Sarna-Wojcicki, A. M., H. R. Bowman, C. E. Meyer, P. C. Russell, M. J. Woodward, Gail McCoy, J. J. Rowe, Jr., P. A. Baedeker, Frank Asaro, and Helen Michael, 1984, *Chemical Analyses, Correlations, and Ages of Upper Pliocene and Pleistocene Ash Layers of East-Central and Southern California*; U. S. Geological Survey Professional Paper 1293, 40 p.
- Sarna-Wojcicki, A. M., C. E. Meyer, H. R. Bowman, N. T. Hall, P. C. Russell, M. J. Woodward, J. L. Slate, in press, *Correlation of the Rockland ash bed, a 450,000 year-old stratigraphic marker in northern California and western Nevada, and implications for mid-Pleistocene paleogeography of central California*; *Quaternary Research*
- Segall, Paul, and Pollard, David, 1983a, *Nucleation and growth of strike-slip faults in granite*; *Journal of Geophysical Research*, Vol., 88, No. B-1, p. 555—568, Jan. 10, 1983.
- Segall, Paul, and Pollard, David, 1983b, *Joint formation in granitic rock of the Sierra Nevada*; *Geological Society of America Bull.*, Vol. 94, No. 5, p. 563—575, May, 1983.
- Shackleton, Nicholas John, and Opdyke, Niel D., 1973, *Oxygen Isotope and Paleomagnetic Stratigraphy of Equatorial Pacific Core V28-238: Oxygen Isotope Temperatures and Ice Volumes on a 10⁵-year and 10⁶-year scale*; *Quaternary Research*, Vol. 3, p. 39—55.
- Shackleton, N. J., and Opdyke, N. D., 1976, *Oxygen-Isotope and Paleomagnetic Stratigraphy of Pacific Core V28-239, Late Pliocene to Latest Pleistocene*; *Geological Society of America Memoir 145*, R. M. Cline and J. D. Hays, eds., *Investigation of Late Quaternary Paleoceanography and Paleoclimatology*, p. 449—464.
- Shackleton, N. J., and Opdyke, N. D., 1977, *Oxygen isotope and paleomagnetic evidence for early Northern Hemisphere Glaciation*; *Nature*, vol. 270, p. 216—219.
- Sharp, Robert P., and Birman, Joseph H., 1963, *Additions to Classical Sequence of Pleistocene Glaciations, Sierra Nevada, California*; *Geological Society of America*

Bulletin, vol. 74, No. 8, p. 1079-1086.

Sisson, Thomas W., and Moore, James G., 1984, Geology of the Giant Forest-Lodgepole area, Sequoia National Park, California; U. S. Geological Survey Open File Report No. 84-254. 24 pages, 1 plate.

Smith, George I., 1976, Paleoclimatic record in the upper Quaternary sediments of Searles Lake, California, U. S. A.; in S. Horie, ed., Paleolimnology of Lake Biwa and the Japanese Pleistocene, vol. 4, p. 577-604.

Smith, George I., 1979, Subsurface stratigraphy and geochemistry of Late Quaternary evaporites, Searles Lake, California, with a section on Radiocarbon Ages of Stratigraphic Units, by Minze Stuiver and George I. Smith; U. S. Geological Survey Professional Paper 1043, 130 pages, 2 plates in pocket.

Smith, George I. in press, Paleohydrologic Regimes in the Southwestern Great Basin, 0-3.2 MY Ago, Compared with other long records of "Global" Climate; Quaternary Research, in press (to be published in 1984).

Smith, George I., Virgil J. Barczak, Gail F. Moulton, and Joseph Liddicoat, 1983, Core KM-3; a Surface-to-Bedrock Record of Late Cenozoic Sedimentation in Searles Valley, California; U. S. Geological Survey Professional Paper 1256, 24 pages, 4 plates in pocket.

Smith, George I., and Street-Perrott, F. Alayne, 1983, Pluvial Lakes of the Western United States; in Late Quaternary Environments of the United States, H. E. Wright, ed., Vol. I, The Late Pleistocene, Stephen C. Porter, ed., p. 190-212, University of Minnesota Press.

Stevens, Rollin E. and Carron, Maxwell K., 1948, Simple field test for distinguishing minerals by abrasion pH; American Mineralogist, Vol. 33, Nos. 1-2, p. 31-49.

Wahrhaftig, Clyde, 1965, Stepped Topography of the southern Sierra Nevada, California; Geological Society of America Bull., Vol. 76, No. 10, p. 1165-1190.

Wahrhaftig, Clyde, and Birman, J. H., 1965, The Quaternary of the Pacific Mountain System in California, in Wright, H. E., Jr., and Frey, D. G., eds., The Quaternary of the United States—a review volume for the VII Congress of the International Association of Quaternary Research; Princeton, N. J., Princeton University Press, p. 299-340.